CHEMICAL REVIEWS

Review

Cite This: *Chem. Rev.* 2020, 120, 434−459

pubs.acs.org/CR

Theory of Nonequilibrium Free Energy Transduction by Molecular Machines

Aidan I. Brown*,† and David A. Sivak*,‡

†Department of Physics, University of California, San Diego, La Jolla, California 92093, United States

‡Department of Physics, Simon Fraser University, Burnaby, British Columbia V5A 1S6, Canada

ABSTRACT: Biomolecular machines are protein complexes that convert between different forms of free energy. They are utilized in nature to accomplish many cellular tasks. As isothermal nonequilibrium stochastic objects at low Reynolds number, they face a distinct set of challenges compared with more familiar human-engineered macroscopic machines. Here we review central questions in their performance as free energy transducers, outline theoretical and modeling approaches to understand these questions, identify both physical limits on their operational characteristics and design principles for improving performance, and discuss emerging areas of research.

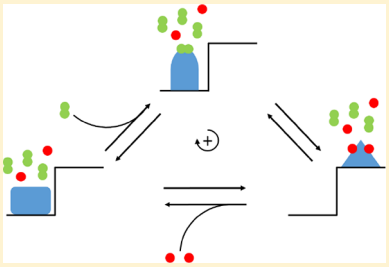

CONTENTS

1. INTRODUCTION

A hallmark of all living things is order, manifested in both structure and dynamical processes. Such order is not possible at equilibrium, where the second law of thermodynamics requires a maximum of disorder, so living things must fundamentally be out of equilibrium.[1] Specifically, cells are characterized by out-of-equilibrium chemical concentrations and inhomogeneous spatial distributions of charge and molecular species.[2,3]

These nonequilibrium conditions are largely created and maintained by molecular machines, i.e., macromolecular complexes that interconvert or transduce different stores (reservoirs) of nonequilibrium free energy. Molecular machines play essential roles in a panoply of core cell-biology

Special Issue: Molecular Motors

Received: April 25, 2019
Published: August 14, 2019

DOI: 10.1021/acs.chemrev.9b00254
Chem. Rev. 2020, 120, 434−459

processes, and their design is an exciting area of ongoing engineering endeavor. To understand biology and unlock future technology, we must understand the principles behind molecular machine operation.

Molecular machines are notably distinct from the macroscopic machines that have been honed by engineers for centuries. The high-level differences result from their nanometer scale and material composition. These and a few other *stylized facts*[a] about the basic features of molecular machine operation provide sufficient constraints to point to relevant simple models and governing physical limits. Stochastic thermodynamics[5,6] is a fruitful and increasingly promising framework within which to understand their operation.

Free energy transduction is a key element in describing how molecular machines work. Because useful molecular machines are in contact with nonequilibrium reservoirs of free energy and material, they are not in equilibrium; the second law of thermodynamics provides guidance, indicating that free energy must be consumed to do useful things.

Here we review theoretical and computational explorations of nonequilibrium free energy transduction in molecular machines. Initial sections of this review lay the groundwork for understanding free energy transduction in molecular machines. Section 2 introduces molecular machine classes and modes of free energy transduction, concluding in section 2.1 with the introduction of two model systems that will be frequent illustrating examples throughout this review. Section 3 summarizes stylized facts that point to considerations for modeling of molecular machine behavior. Section 4 outlines the basic elements of popular modeling approaches and section 5 the kinetic and thermodynamic concepts that figure prominently in such models. Section 6 describes common measures of performance that quantitatively describe the functionality of molecular machine operation, example values from various molecular machines, and how machine characteristics can lead to improved performance. Subsections of section 6 discuss in more detail several frameworks for analyzing and computing molecular machine free energy transduction, with focuses on how free energy is consumed to generate autonomous and reliable directed machine behavior, molecular machine features that lead to fast and efficient operation, and trade-offs between various performance measures. Section 7 covers the energetic costs incurred by control protocols. Although we focus primarily on naturally evolved biomolecular machines, section 8 briefly discusses insights gained from and possible applications to synthetic molecular machines. Section 9 outlines several areas of emerging and future interest. Section 10 finishes with some concluding thoughts.

We focus on recent literature, though of necessity we refer back to earlier work to introduce relevant frameworks, models, and questions. We also refer the reader to an excellent set of reviews in previous years on various aspects of molecular machine operation and modeling from a theoretical perspective.[5,7−21]

2. TYPES OF MOLECULAR MACHINES

Biomolecular machines fulfill a wide variety of cellular roles.[15] At their most fundamental, each type of molecular machine transduces one nonequilibrium store of free energy into another, converting among mechanical energy, electrical energy, chemical energy, and low-entropy distributions both across space and among chemical species (small molecules and biopolymer sequences).

Transport motors[b] (e.g., kinesin,[22] dynein,[23] and myosin[24]) haul cellular cargoes (e.g., organelles or chromosomes) along cellular filaments,[25] thereby transducing chemical potential differences (often between ATP and ADP + inorganic phosphate (P_i)) into directed mechanical forces and ultimately into spatial concentration differences. Translocases (e.g., the ϕ29 packaging motor[26] and nucleic-acid helicases[27]) pull biopolymers (during packaging or unwinding), thereby transducing chemical potential differences into mechanical forces and ultimately high pressures (packaging motors) or redistribution across free energy barriers. Muscle motors (e.g., myosin in actomyosin fibers[3]) provide motion in muscles, thereby transducing chemical potential differences into linear movement against loads (i.e., performing work). Pumps (e.g., Na^+/K^+-ATPase[28] and electron-transport complexes I, III, and IV in cellular respiration[3]) push small molecules across membranes, thereby transducing chemical potential differences between reactants and products into concentration differences of another chemical species across membranes. Polymerases (DNA polymerase,[29] RNA polymerase,[30] and the ribosome[31]) add monomers to the ends of biopolymers, thereby transducing chemical potential differences into low-entropy distributions of polymer sequences. Rotary motors (e.g., F_OF_1-ATP synthase[32] and the bacterial flagellum[33]) transduce electrochemical differences across membranes into rotation against a torque (and thus perform work).

Molecular machines often work as part of tightly or loosely coupled larger assemblies to accomplish their functions: transport motors can work together (and antagonistically, when oppositely directed) to transport cargoes;[34,35] F_OF_1-ATP synthase is an intimate assembly of two oppositely directed rotary motors;[32] polymerase holoenzymes include core polymerases, helicases, and error-checking apparatus;[3,36] and actomyosin fibers consist of precise spatial arrangements of myosin motors.[3]

2.1. Case Studies

When illustrating the concepts in this review, we focus on two molecular machines, ATP synthase and kinesin. Despite this special emphasis, the ideas in this review apply beyond these two examples to other machines and to systems sometimes not considered as molecular machines,[37] such as catalytic enzymes.[38]

ATP synthase couples transport of hydrogen ions down their gradient to the synthesis of ATP from ADP + P_i against a chemical potential difference favoring ATP hydrolysis.[32] Though ATP synthase is a large and intricate molecular complex, communication is mediated through a relatively simple mechanical coordinate, the rotational angle of a crankshaft connecting the integral membrane F_O subunit to the soluble F_1 subunit (Figure 1). Single-molecule studies of ATP synthase typically remove the F_O subunit, attach an experimental handle (e.g., a single magnetic bead or dimeric beads) to the crankshaft attached to the F_1 subunit, and monitor or force rotation using a magnetic trap[39] or electrorotation.[40] Such experiments suggest that F_1 can approach near 100% efficiency.[39−42]

Kinesin-1 (hereafter kinesin) is a transport motor that walks toward the plus end of microtubules, powered by ATP hydrolysis.[52,53] Kinesin takes discrete 8 nm steps[54] as its two "heads" alternate binding in a hand-over-hand fashion along the microtubule.[55] These heads contribute much of the activity necessary for kinesin walking, including binding to the

DOI: 10.1021/acs.chemrev.9b00254
Chem. Rev. 2020, 120, 434−459

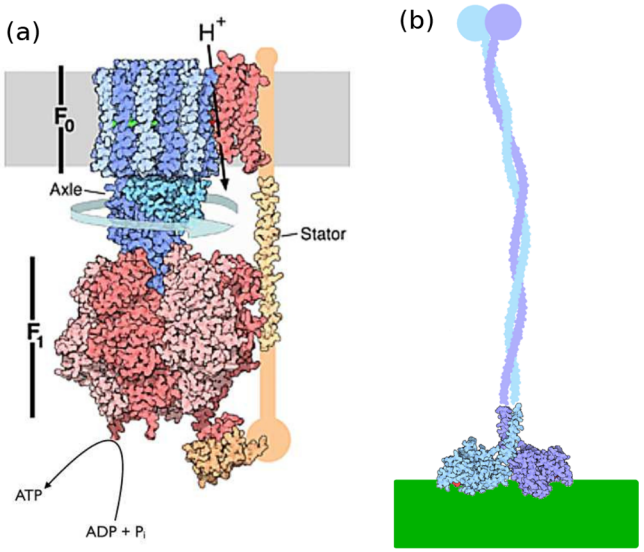

Figure 1. Model systems. (a) ATP synthase (~10 nm in diameter[43]), a composite rotary motor. The membrane-embedded F_O motor (top, blue) couples proton flow across the membrane (down the electrochemical gradient) to rotation of the central axle or crankshaft. The cytoplasmic F_1 motor (bottom, red) couples this rotation to the synthesis of ATP from ADP + P_i. (b) Representation of the crystal structure of kinesin, a motor that walks along microtubules (shown in green), towing cellular cargo. The ~7 nm diameter[44] motor domain at the bottom (where microtubule binding and ATP hydrolysis occur) is connected via an ~80 nm linker[45] to the cargo-binding domain on top (shown schematically). Both images adapted from the Protein Data Bank.[46−51]

microtubule, hydrolyzing ATP, and gating their enzymatic activity to provide directed motion.[56] The two heads are connected to a "neck linker", which provides important conformational changes as part of the kinesin stepping cycle.[57,58] The neck linker is also connected to a longer coiled coil that ends in a cargo-binding domain[59] (Figure 1). In addition to its main forward stepping pathway, kinesin can take backward steps (requiring ATP hydrolysis) and engage in futile cycles that hydrolyze ATP without taking a step in either direction.[60] Kinesin can take many forward steps before detaching from a microtubule.[61] By attachment of a bead to kinesin, an optical trap can manipulate kinesin by applying force as it walks.[60]

3. STYLIZED FACTS

Here we outline stylized facts about the unfamiliar, often counterintuitive, physical setting for molecular machines. Overall, the considerations in this section suggest that nonequilibrium and statistical approaches applied to isothermal, overdamped, thermodynamically consistent models that properly account for mechanical and chemical degrees of freedom are central to understanding the behavior and design of molecular machines.

Molecular machines are of necessity isothermal machines. Any temperature gradient sufficiently large and on sufficiently short length scales to power meaningful motion of a molecular machine would relax long before the machine could complete a cycle.[17,62]

These nanometer-sized objects, composed of relatively soft protein material, have energy scales comparable to the thermal energy k_BT at ambient temperature, so significant stochastic fluctuations are omnipresent.[63,64] Similar to pollen grains diffusing in water,[65] the components of molecular machines (unlike macroscopic machines) experience large stochastic fluctuations as they are constantly jostled by collisions with the surrounding medium (typically water or other proteins). Thus, even a driven molecular machine will move in a given direction only on average, with pauses, back steps, off-pathway (side) steps, and so on.[66] These stochastic fluctuations are another manifestation of the noise that frictionally damps molecular machine motion: at equilibrium, the frictional damping and stochastic kicks are tightly connected by the fluctuation−dissipation theorem.[67,c]

The typical length and velocity scales of molecular machines place them in the regime of low Reynolds number,[71] $Re \equiv vL/(\mu/\rho)$, for velocity v, characteristic linear dimension L, viscosity μ, and mass density ρ. Kinesin has a maximum speed of ~1 μm/s and a size of ~10 nm, and room-temperature water has viscosity of ~10^{-3} Pa·s and an approximate density of 10^3 kg/m^3, suggesting a Reynolds number of Re ~ 10^{-8}.[72] Thus, viscous (frictional) forces dominate inertial forces, so the motion of molecular machines is completely overdamped: any instantaneous direction of motion is rapidly randomized by energetic collisions with the machine's surroundings. As a result, a molecular machine rapidly "forgets" its direction of motion. Unlike a macroscopic machine, a molecular machine cannot rely on inertia to carry it through any particular stage of its cycle. The average motion of such nanoscale objects persists only as long as something continues to "push". Essentially, any machine "velocity" emerges only from an imbalance of forward versus backward steps, not from any physically meaningful instantaneous velocity.

Molecular machines operate in the crowded environment of the cellular interior.[73−75] Water has a viscosity of 10^{-3} Pa·s, while viscosity measurements inside the cell reach as high as 10^3 Pa·s, a million-fold higher.[76] This higher intracellular viscosity is due to *macromolecular crowding*, i.e. the high concentrations of macromolecules, which occupy 10−40% of the cell volume.[77] This suggests that the Reynolds number experienced by biomolecular machines is substantially smaller than even the low value they would experience in water.

Molecular machines typically operate cyclically,[d] allowing repetition of a task, with stochastic behavior on shorter time scales averaging to more reliable output on longer time scales. These machine cycles involve events with both chemical and conformational changes. Chemical reactions and ligand binding/unbinding events proceed essentially instantaneously compared with conformational relaxation time scales, but waiting times for chemical reactions can exceed conformational relaxation time scales.

Molecular machines are often assembled from many components. These components are strongly coupled and interact with different aspects of their environment. The emerging field of stochastic thermodynamics of strongly coupled systems provides promising frameworks[79−82] to investigate free energy transduction among the various components of machines.

The elasticity of the coupling between different machine components allows energy to be elastically stored and perhaps accumulated at an interface before release, essentially smoothing any mismatches between interacting components. This permits kinetic decoupling of the behavior of two interacting machines.[32] For example, in F_OF_1-ATP synthase,

DOI: 10.1021/acs.chemrev.9b00254
Chem. Rev. 2020, 120, 434−459

elastic energy storage may permit the transmission of energy between components that have different periodicities, such as F_O and F_1.[83−89]

3.1. Microscopic Reversibility and Nonequilibrium Driving

Molecular machines, with overdamped motion and jostled by fluctuations, can nonetheless complete the stages composing their operational cycles. Microscopic reversibility[90,91] dictates that for every trajectory that completes a molecular machine stage in the forward (functional) direction, there must be a corresponding physically realizable reverse (dysfunctional) trajectory. Any forward step must be matched by the potential for a backward step, however unlikely. Thus, the operation of any molecular machine is in principle microscopically reversible, capable of reversing any free energy conversion to run in the opposite direction, though the reverse operation may be so unlikely as to be unobserved in a given experiment. Hence, it is of necessity a probabilistic phenomenon, not a deterministic one. This (mechanical and chemical) reversibility has actually been experimentally demonstrated[13] for F_1-ATPase[39,40] the full F_OF_1-ATP synthase,[92] and an isolated stage of the kinesin cycle.[93,e]

At thermal equilibrium, microscopic reversibility and the resulting detailed balance[97] require zero net flux between different states. Hence, molecular machines at equilibrium are not functional and do no useful work: a transport motor at equilibrium is as likely to take backward steps as forward steps; F_OF_1-ATP synthase at equilibrium is equally likely to hydrolyze or synthesize ATP.

This immediately implies that molecular machines must be out of equilibrium in order to be functional. It is fundamental to the operation of molecular machines—and the directed behavior they must achieve—that they operate out of equilibrium. The ability of a molecular machine to achieve directed motion relies on driving by nonequilibrium forces, which necessarily dissipate free energy.

This requirement of free energy for directed behavior is illustrated by Feynman's ratchet and pawl[98] (Figure 2), which describes a wheel with asymmetric teeth that has its rotation in one direction (counterclockwise, without loss of generality) limited by a pawl. The wheel is coupled to a vane to introduce fluctuations, with the stochastic impact of gas molecules occasionally driving the wheel clockwise. This scenario appears to violate the second law of thermodynamics, as thermal gas molecule fluctuations drive directed rotation of the wheel. The second law in fact holds because the same fluctuations that drive rotation in the clockwise direction also disengage the pawl, allowing counterclockwise motion, and thus, as a whole the thermal fluctuations do not produce net average rotation in either direction.[99]

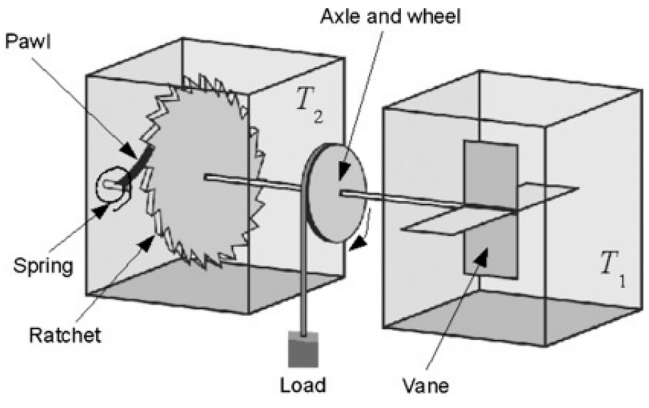

Figure 2. Feynman's ratchet and pawl. A vane rotationally fluctuates from impact with diffusing gas molecules. The vane rotates a ratchet (with asymmetric teeth) that has a pawl to prevent rotation in the "wrong" direction when held down by a spring. If the vane and ratchet rotate in the correct direction, the device can do useful work by lifting a load. Reproduced with permission from ref 100. Copyright 2008 Institute of Physics.

There are two requirements to rectify thermal fluctuations into directed motion and hence potentially into mechanical work:[12] spatial asymmetry and nonequilibrium driving.[17] Nonequilibrium driving provides temporal asymmetry to molecular machine dynamics, and spatial asymmetry permits a directed response to free energy input.

The free energy consumed by molecular machine operation but not transduced into another store of free energy is known as dissipation. Although some molecular machines are quite efficient and convert between forms of free energy in such a way that most of the free energy from the fuel is later available for some other process, other machines dissipate much of the free energy from fuel. For example, under physiologically relevant conditions, kinesin dissipates most of its input free energy.[101] This dissipated free energy provides forward bias (see section 5.3). At macroscopic scales, this free energy cost of directionality is also present but can be much smaller in comparison with the total free energy input.[102]

In contrast to heat engines driven by temperature differences, biomolecular machines are isothermal and instead driven by nonequilibrium chemistry, typically from nonequilibrium concentrations of reactants and products or gradients maintained across membranes. Many machines are driven by ATP hydrolysis; in physiological contexts, the concentrations of ATP and its hydrolysis products ADP + P_i are maintained out of equilibrium so that they provide a $20k_BT$ driving force,[103] dwarfing the scale of thermal fluctuations.

The directionality imposed by out-of-equilibrium concentrations of chemical species depends on the likelihood that particular species will bind to the machine. Only those kinetic steps involving binding of chemical species are sensitive to the concentrations of those species. In particular, conformational changes that do not change the binding state of a machine are not biased by chemical potential driving forces.[91]

4. MODELS

Given the qualitative regimes describing molecular machines in section 3, many researchers have developed simple models for molecular machine energetics and dynamics in order to gain understanding. To be analytically tractable, models of molecular machines typically have few degrees of freedom. These degrees of freedom include mechanical or conformational variables, binding and unbinding reactions (to ligands or cytoskeletal filaments), and chemical degrees of freedom.

4.1. Continuum Models

Molecular machine dynamics can be modeled as diffusion on an energy landscape with a continuous state space. For a given generalized machine coordinate $\mathbf{x}$, the energy is $V(\mathbf{x})$. The machine moves on the energy landscape with a rapidity depending on the diffusivity $D(\mathbf{x})$, which is often assumed to be uniform.

The system dynamics is typically analytically or numerically solved using one of two primary approaches: solving for the

DOI: 10.1021/acs.chemrev.9b00254
Chem. Rev. 2020, 120, 434−459

temporal evolution of the probability distribution using the Fokker–Planck equation[104] or simulating realizations of individual trajectories using Monte Carlo or Langevin methods.[97,105−109]

Often the multidimensional state space of the molecular machine is reduced to a single coordinate x along which reaction progress in the "forward" direction is considered (Figure 3). Averaging over other degrees of freedom

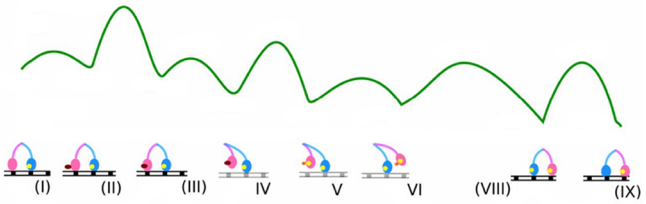

Figure 3. Continuous free energy landscape. Top: Free energy landscape for a single step of myosin-V on an actin filament. Bottom: Schematic progression of myosin-V states (sequentially labeled with Roman numerals) aligned with the locations of the corresponding metastable states along the free energy landscape. Adapted from ref 111.

(presumed to relax faster) is performed using a time scale separation argument[110] to arrive at the free energy $V_{\text{eff}}(x)$ and diffusivity $D_{\text{eff}}(x)$ along this single coordinate.

Multiple model types can describe the generation of directed behavior in molecular machine models. Here we outline two such models.

One is a *flashing potential*, which instantaneously switches between multiple free energy landscapes[112] (Figure 4). The

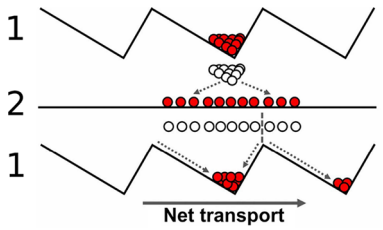

Figure 4. Flashing ratchet generating directed behavior through alternation between two potentials. In the sawtooth potential (1), the machine generally localizes to the bottom of the free energy wells (red particles represent an ensemble of final machine positions in potential). When the potential switches to the flat potential (2), the ensemble of initial machine positions (represented by white particles) then diffuse isotropically (with the final machine positions again represented by red particles). When the potential flashes back to the sawtooth potential (initial machine positions shown as white particles), machines that have reached a neighboring free energy well tend to relax to the bottom of that well rather than returning to the initial well. Diffusion is isotropic, but because the free energy wells are asymmetric, the machine is more likely to reach the basin of a neighboring well to the right rather than to the left. On average, the machine makes directed progress. Adapted from ref 113.

alternating potentials are chosen such that on average this switching will drive the machine in one direction. A typical scenario involves two features: energy landscapes whose periodic features are not aligned and sufficiently long wait times between switches to allow the machine time to find an energy minimum. Figure 4 shows how isotropic diffusive spreading can be rectified by asymmetric energy wells as part of a flashing potential.

Another standard model involves periodic repetition of the entire landscape representing the machine cycle, with an overall free energy drop over the course of the entire cycle, such that the landscape is "tilted".[114] As the machine diffuses on the free energy landscape, it will tend to move toward lower free energy, generating directed behavior in that direction.[106]

4.2. Discrete-State Models

Alternatively, the state space of molecular machines is often divided into a set of discrete states[115] (Figure 5). This discrete-

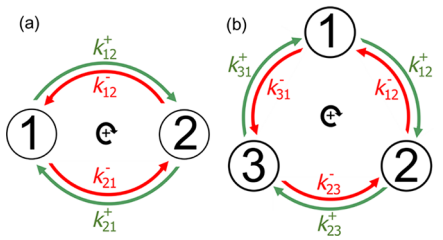

Figure 5. Discrete-state models with (a) two and (b) three states per cycle. Transitions occur in both the forward (green arrows) and reverse (red arrows) directions for each pathway, with respective rate constants k_{ij}^{+} and k_{ij}^{-}. Reproduced from ref 137. Copyright 2018 American Chemical Society.

state description is motivated by the commonly encountered situation of large barriers separating compact metastable macrostates, in which a time scale separation exists between relatively long time scales spent within a given macrostate and relatively short time scales to actually make the transition between macrostates.[116]

In a discrete-state model, k_{ij}^{+} is the transition rate constant in the forward direction from state i to state j, and k_{ij}^{-} is the reverse transition rate constant from state j to state i along the same transition path. This description allows for physically distinct pathways between two states that, though they begin in the same state and finish in the same state, have distinct effects on the environment. For example, in Figure 5, k_{12}^{+} and k_{12}^{-} could be the respective rates of phosphorylation and dephosphorylation by ATP-driven enzymatic catalysis and k_{21}^{+} and k_{21}^{-} the respective rates of undriven nonenzymatic dephosphorylation and phosphorylation.

A continuous model can incorporate more details in the free energy landscape and allow the assessment of behavior during transitions, but discrete-state models can more computationally efficiently generate trajectories and dynamic probability distributions.

4.3. Hybrid Models

Continuous and discrete-state molecular machine models can be combined in models that feature discrete transitions between multiple continuous free energy landscapes[117] (e.g., Figure 6). This combination permits the use of discrete or continuous descriptions of different degrees of freedom as appropriate. For example, though the waiting time between chemical reactions can be long, the actual transition time is typically much shorter than characteristic time scales for protein conformational rearrangements, so a chemical reaction can be modeled as a discrete transition between continuous mechanical landscapes.

DOI: 10.1021/acs.chemrev.9b00254
Chem. Rev. 2020, 120, 434−459

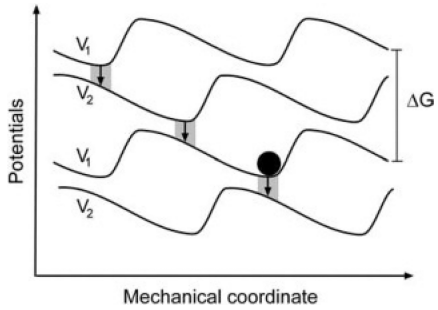

Figure 6. Hybrid model. Schematic continuous free energy landscapes connected by discrete transitions between distinct landscapes from a particular location on each landscape. Reproduced with permission from ref 118. Copyright 2005 The Biophysical Society.

A flashing potential is an example of a hybrid model that typically transitions between potentials independently of the machine state. Instead, the potentials alternate on a set schedule.

4.4. Atomistic or Coarse-Grained Molecular Models

More detailed computational models either explicitly represent all atoms[89,119−121] or coarse-grain individual atoms into larger effective particles.[122−124] The number of degrees of freedom and complexity of force fields preclude any analytic treatments, so these models are solved using discrete integration of equations of motion, either deterministic or stochastic.[107] Such models can incorporate significantly more molecular detail and potentially resolve the ramifications of such details on machine performance, but their increased computational cost limits the accessible simulation time scales and reduces the breadth of statistical sampling.

5. BACKGROUND QUANTITATIVE CONCEPTS

Given the roles of molecular machines (section 2), the qualitative environment that they encounter (section 3), and the models used to describe their dynamics (section 4), we now outline some quantities and properties that are important for understanding molecular machine behavior.

5.1. Flux

The macrostate of a molecular machine is often described using the probability distribution across microstates. For a discrete-state model, in which the probability of occupying a given discrete microstate i is P_i, the directed (one-way) probability flux from state i to state j along a given pathway is

$$J_{ij}^{+} = k_{ij}^{+} P_i \tag{1}$$

and that from state j to state i is

$$J_{ij}^{-} = k_{ij}^{-} P_j \tag{2}$$

The net flux, i.e., the net flow of probability from state i to state j along a given pathway, is the difference of the directed fluxes:

$$J_{ij} = J_{ij}^{+} - J_{ij}^{-} = k_{ij}^{+} P_i - k_{ij}^{-} P_j \tag{3}$$

A system at equilibrium satisfies *detailed balance*, where for each pathway $i \rightleftarrows j$ the "forward" flux J_{ij}^{+} from i to j is exactly balanced by the "reverse" flux J_{ij}^{-} from j to i:

$$k_{ij}^{+} P_i = k_{ij}^{-} P_j \tag{4}$$

Therefore, at equilibrium,

$$J_{ij} = 0 \tag{5}$$

5.2. Nonequilibrium Steady State

For constant external conditions, a machine can reach a *nonequilibrium steady state* (NESS) in which for each state the total incoming and outgoing fluxes balance:

$$\sum_j (J_{ij}^{+} - J_{ij}^{-}) = 0 \quad \forall\, i \tag{6}$$

The distinction of a NESS from equilibrium is that the state probabilities do not necessarily satisfy the detailed balance condition (eq 5), for which each and every individual flux balances. Although in a NESS the state probabilities remain constant over time, these probabilities do not generally satisfy the Boltzmann distribution.[125] We will primarily consider machines in a NESS, as any long-term averages should be dominated by NESS behavior and only marginally affected by transient behavior during relaxation to a NESS.

For a discrete-state model that has reached a NESS, the flux can be calculated using Hill's diagrammatic method.[126] This approach gives the NESS flux for a two-state cycle (Figure 5a) as

$$J_{\text{two-state NESS}} = \frac{k_{12}^{+}k_{21}^{+} - k_{12}^{-}k_{21}^{-}}{k_{12}^{+} + k_{12}^{-} + k_{21}^{+} + k_{21}^{-}} \tag{7}$$

and that for a three-state cycle (Figure 5b) as

$$\begin{aligned} J_{\text{three-state NESS}} = {} & (k_{12}^{+}k_{23}^{+}k_{31}^{+} - k_{12}^{-}k_{23}^{-}k_{31}^{-}) \\ & /(k_{12}^{+}k_{23}^{-} + k_{12}^{-}k_{23}^{-} + k_{23}^{-}k_{31}^{-} + k_{12}^{+}k_{31}^{+} \\ & + k_{12}^{-}k_{31}^{+} + k_{12}^{-}k_{31}^{-} + k_{12}^{+}k_{23}^{+} + k_{23}^{+}k_{31}^{+} \\ & + k_{23}^{+}k_{31}^{-}) \end{aligned} \tag{8}$$

Generating-function methods[127−129] are a popular alternative to the diagrammatic method. NESS fluxes for models with more states or multiple cycles can also be calculated via either method, but the expressions quickly become unwieldy.

5.3. Free Energy

The dissipated free energy ω_{ij} is related to the bias of transition rate constants through the *generalized detailed balance* condition:

$$\beta\omega_{ij} = \ln \frac{k_{ij}^{+}}{k_{ij}^{-}} \tag{9}$$

where $\beta \equiv (k_B T)^{-1}$. For an autonomous molecular machine, ω_{ij} is the free energy dissipation cost paid for biased forward progress at discrete transition $i \rightarrow j$. This dissipated free energy ω_{ij} is the height of the downhill drop the machine experiences over the transition, as dissipated energy is not subsequently available to perform useful work. The forward bias provided by ω_{ij} is often described as "driving" the machine.

5.4. Control-Parameter Protocol

An equilibrium ensemble can be parametrized by a control parameter λ manipulated by an experimentalist. Molecular machines are often experimentally probed by temporal variation of control parameters such as the distance between foci of optical traps[130] or the rotational angle of a magnetic trap.[39] A *protocol* Λ specifies a temporal driving schedule for changing the control parameter $\lambda(t)$ from the initial value λ_i to the final value λ_f in some specified time.

DOI: 10.1021/acs.chemrev.9b00254
Chem. Rev. 2020, 120, 434−459

5.5. Affinity

For a molecular machine driven by constant nonequilibrium external conditions, the *affinity* ω_{tot} is the total amount of free energy driving forward progress per cycle, given by the sum of the free energies dissipated during the individual transitions:[16,131]

$$\omega_{tot} = \sum \omega_{ij} \tag{10}$$

where ω_{ij} is given by eq 9. Molecular machine models with multiple cycles (e.g., kinesin models[60] with back steps and futile cycles) have a distinct affinity for each cycle.

The affinity is equivalently related to the ratio of the product of all forward transition rate constants to the product of all reverse transition rate constants around a machine cycle:[16]

$$\beta\omega_{tot} = \ln \frac{\prod_{i=1}^{N} k_{ij}^{+}}{\prod_{i=1}^{N} k_{ij}^{-}} \tag{11}$$

For a system experiencing only chemical driving, the maximum affinity is equal to the negative of the free energy change for conversion of chemical reactants to products. For hydrolysis of ATP into ADP + P_i, the maximum affinity is given by the sum of the intrinsic free energy change ΔG_0 for the reaction and the logarithm of the ratio of nonequilibrium concentrations:

$$\omega_{tot}^{max} = \Delta G_{ATP\ hydrolysis} = \Delta G_0 + k_B T \ln \frac{[ADP][P_i]}{[ATP]} \tag{12}$$

The maximum affinity ω_{tot}^{max} in eq 12 is the free energy available for the molecular machine both to dissipate and to transduce to another free energy reservoir. The affinity in eqs 10 and 11 is the free energy dissipated by the molecular machine. The difference, $\omega_{tot}^{max} - \omega_{tot}$, is the free energy transduced from the fuel to another free energy reservoir, e.g., moving an ion from low concentration to high concentration.

5.6. Microscopic Reversibility

At equilibrium, system dynamics must satisfy detailed balance (eq 5), with the forward flux for any pathway exactly balanced by the reverse flux for that pathway. Implicit in the concept of detailed balance is the idea that any forward trajectory must have a corresponding reverse trajectory that is in principle possible, including when the system is not at equilibrium.[90,91] This principle of *microscopic reversibility* is manifested in the construction of thermodynamically consistent models by the requirement that for each forward transition there must be a corresponding reverse transition.

Although the reverse of a particular microscopic process is always possible, it is not necessarily likely. The Crooks fluctuation theorem describes the relative likelihood of forward and reverse trajectories in terms of the entropy production along the forward trajectory:[132]

$$\frac{P[x(t)]}{\tilde{P}[\tilde{x}(t)]} = e^{\sigma[x(t)]/k_B} \tag{13}$$

where $P[x(t)]$ is the probability of the forward trajectory $x(t)$, $\tilde{P}[\tilde{x}(t)]$ is the probability of the time-reversed trajectory $\tilde{x}(t)$, and $\sigma[x(t)]$ is the entropy produced by trajectory $x(t)$.

According to the Crooks fluctuation theorem, the ratio of the respective probabilities for a forward trajectory and the corresponding reverse trajectory exponentially increases with the entropy produced. The Crooks fluctuation theorem (eq 13) has a similar form as the generalized detailed balance condition (eq 9) for discrete transitions; both eq 9 and eq 13 describe how increasing dissipation decreases the likelihood of a reverse process relative to the forward process.

Given the centrality of fluctuation theorems (from Crooks and others) to stochastic thermodynamics and the fundamentally stochastic nonequilibrium operation of molecular machines, many have emphasized the importance of fluctuation relations in understanding machine operation.[133]

5.7. Splitting Factor

The generalized detailed balance condition (eq 9) dictates the relation between the ratio of the forward and reverse transition rates and the free energy dissipation, but it does not fix the absolute rates and hence leaves unspecified how the forward and reverse rates vary with the model parameters.

For discrete-state models, the transition rates coarse-grain details about the underlying continuous free energy landscape. How much the dissipation affects the forward and reverse transition rates when the dissipation is varied relates to details of the free energy landscape. For example, in Figure 7 two states are separated by a distance l, with the transition state a distance δl in front of the rear state (to the left) and a distance $(1 - \delta)l$ behind the front state (to the right).[134−136]

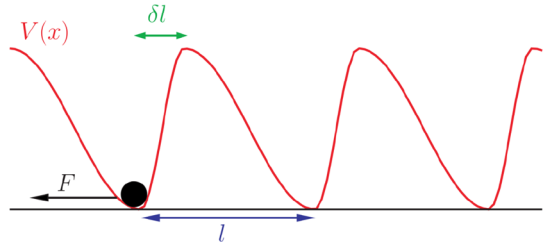

Figure 7. Splitting factors. Shown in red is the free energy landscape $V(x)$ for a molecular motor taking steps of size l opposed by a force F. The transition state is positioned a fraction δ of the total step size l between adjacent metastable states (i.e., a distance δl from the state to the left and a distance $(1 - \delta)l$ from the state to the right). Reproduced with permission from ref 134. Copyright 2008 European Physical Society.

The splitting (or load-distribution) factor δ divides the forward bias among the forward and reverse rate constants:[137]

$$k_{ij}^{+} = k_{ij}^{0} e^{\beta\delta\omega_{ij}} \quad \text{and} \quad k_{ij}^{-} = k_{ij}^{0} e^{-\beta(1-\delta)\omega_{ij}} \tag{14}$$

where k_{ij}^{0} is the bare rate constant that describes the inherent rate of the $i \rightleftarrows j$ transition at equilibrium, combining barrier height and diffusivity along the free energy landscape. The splitting factors can also be distinct for different free energy terms for a transition, e.g., the "intrinsic" free energy change of the machine in a given environment and the energy change due to motion against an applied force.[137]

The applied force in Figure 7 acts as an additional constant-gradient contribution to the energy landscape (effectively imparting a tilt to the left). If δ approaches zero, the transition state is close to the rear state, and this constant gradient adds little to the free energy hill the machine must climb to complete the forward transition (slightly decreasing k_{ij}^{+} in eq 14) but substantially decreases the hill the machine must climb to reverse the transition (substantially increasing k_{ij}^{-} in eq 14). In contrast, if δ approaches 1, the transition state is close to the front state, and the constant gradient substantially increases the

DOI: 10.1021/acs.chemrev.9b00254
Chem. Rev. 2020, 120, 434−459

hill in the forward direction (substantially decreasing k_{ij}^{+} in eq 14) and only slightly decreases the hill in the reverse direction (slightly increasing k_{ij}^{-} in eq 14).

5.8. Power Stroke and Brownian Ratchet

Above we outlined how splitting factors describe the effect of dissipation on the forward and reverse rate constants. A closely related concept is the mechanism by which the consumption of free energy produces directed molecular machine operation. This has frequently (including recently[17,136,138]) taken the form of a contrast between *power strokes* and *Brownian ratchets*. Here we survey the characteristics used to describe these two mechanisms.

A power stroke is a conformational change between two mechanical states,[138] possibly driven by strain[139] or stored elastic energy.[12,17] Mechanical transitions with power-stroke mechanisms have been described as directly driven by chemical binding, reaction, or release.[9,139,140] These chemical processes powering the machine cycle do not need to immediately precede the power-stroke transition—the free energy dissipation provided by the reaction of chemical fuel to form products can be spread over a machine cycle and used at distinct transitions. A power stroke has a transition state relatively near the pre-power-stroke state and relatively far from the post-power-stroke state,[139] leading loads to primarily affect the reverse rates and leave the forward rates relatively unchanged.[136] Power strokes are typically seen as decreasing free energy, but alternative voices argue that the opposite is possible.[138]

Mechanisms that use free energy to rectify fluctuations that have made forward progress (by adjusting barrier heights afterward, possibly through chemical binding or reaction) and do not perform work as part of specific conformational changes are described as Brownian or thermal ratchets.[9,12,140] Strain that develops in a Brownian ratchet mechanism is due to thermal fluctuations rather than a specific chemical transition.[139] A Brownian ratchet has a transition state relatively far from the initial state and close to the final state (in the forward direction of the machine cycle), such that the loads primarily affect the forward rates and leave the reverse rates relatively unchanged.[136]

Power strokes and Brownian ratchets have sometimes been presented in the literature as if they are mutually exclusive mechanisms for driving molecular machines. However, individual transitions of a molecular machine can reasonably be said to mix these two mechanisms,[17,141] and different mechanisms can operate at different stages of the same molecular machine.[9]

For the low Reynolds number dynamics of molecular machine components, the mean velocities are proportional to the applied forces. Accordingly, the traditional power-stroke picture, where the development of physical strain drives a conformational change of the machine, requires sustained applied force (i.e., a trajectory with a continuously decreasing potential). With such dynamics that are entirely driven and lack a significant diffusive contribution, a system naturally gravitates toward a local minimum, thereby struggling to reach a specific low-free-energy state in a rugged landscape.[17] Although some well-studied biomolecular machine transitions may indeed be well-described by a traditional power-stroke model (e.g., muscle myosin appears to involve force on a lever arm[142]), many conformational changes are likely to adjust the free energy landscape experienced by some other component of the molecular machine, thereby facilitating a Brownian transition. Binding, reaction, and release of chemicals appear to often alter the free energy landscape experienced by the molecular machine rather than directly provide forces.[117,143−146] This description of machine driving, with the free energy landscape altered by discrete chemical transitions, belongs to the hybrid model type (section 4.3).

5.9. Linear Response

Linear response theory[67,147] represents a popular first-order theoretical framework for near-equilibrium systems. It expresses the system response as a linear function of nonequilibrium driving forces and dynamic control parameter changes.[148] Linear response provides a satisfactory approximation for sufficiently slow protocols or sufficiently mild driving forces. As a first-order theory, linear response offers tractability and generality independent of many system-specific details but sacrifices accuracy far from its applicable limits.

6. MEASURES, LIMITATIONS, AND OPTIMIZATION OF PERFORMANCE

There are many criteria to assess the performance of a molecular machine, of which some (e.g., efficiency, speed, power, and stall force) are familiar from the analysis of macroscopic machines and others (e.g., precision, processivity, and specificity) are distinctive to the fundamentally stochastic behavior of molecular machines. We outline a set of measures that are in principle important to a wide array of molecular machines, though the particular functional tasks and physiological context of a given machine may mean that there are no selective pressures to improve a particular measure.

Here we also provide a sampling of empirical observations of these measures of performance in order to give an overview of molecular machine capabilities and how they behave in practice. Many of these observations motivate the development of theoretical frameworks to understand how closely molecular machine performance approaches physical limits and how that is achieved. There is significant interest in determining which machine designs lead to high performance because of both the insight it may yield to the functioning of living systems (where the presumptive selective advantage of better performance could plausibly lead to the evolution of high-performance machines) and the guidance it can provide to the engineering of novel molecular machines.

Finally, we also describe how machine characteristics can lead to improved performance.

6.1. Efficiency

Although there is not a single universal definition of *efficiency* (η), it is commonly defined as the fraction of input free energy converted to output free energy, and we first discuss this free-energetic efficiency.

Heat engines in contact with a hot heat bath at temperature T_h and a colder heat bath at temperature T_c (i.e., $T_h > T_c$) have efficiencies bounded by the Carnot limit, $1 - T_c/T_h$, which is achieved only with infinitely slow engine operation.[149] The efficiencies of molecular machines, which operate isothermally and are often driven by chemical potentials, are not meaningfully restricted by the Carnot limit. For molecular machines with tight coupling between consumption of chemical fuel and motion (i.e., the machine cycle and fuel consumption cannot occur separately), high efficiency—even approaching unity—can be achieved.[9,150,151] However, near

DOI: 10.1021/acs.chemrev.9b00254
Chem. Rev. 2020, 120, 434−459

stall these tightly coupled machines have low flux and power.[9,151] Multicyclic or loosely coupled machines have lower efficiencies than tightly coupled machines.[151] For machines with multiple stages, the highest efficiency is achieved when the machine driving force is nearly constant.[152,153]

Since the high efficiencies achieved near stall force with very low flux do not reflect typical molecular machine operation, the efficiency is often considered at maximum power.[134] The achievable efficiency depends on the driving regime, with low driving (low dissipation per machine cycle) distinct from greater driving. For sufficiently low driving (i.e., with dissipation $\ll k_BT$), the machine operates in the linear-response regime, universally achieving an efficiency at maximum power of $^1/_2$ for tightly coupled machines.[134,154] For greater driving, beyond the linear-response regime, the efficiency can exceed $^1/_2$[151] depending on the splitting factor δ (representing the transition state location).[134,154] Even for a loosely coupled motor, the efficiency at maximum power is maximized at $\delta = 0$,[134] corresponding to a transition state near the initial state rather than the final state.[134,136,154]

Because of the stochastic dynamics of molecular machines, their efficiency is often considered as an average over many trajectories. The efficiencies of individual trajectories are subject to fluctuations and can be negative or even exceed 1, although these fluctuations (inaccessible in macroscopic systems) are unlikely.[155,156]

When the only output is work against an external force (f_{ext}), the efficiency is[134,150,157,158]

$$\eta = \frac{f_{ext} v}{J\Delta\mu} \tag{15}$$

in which v is the velocity, J is the flux, and $\Delta\mu$ is the change in chemical potential per cycle (i.e., the affinity ω_{tot} at $f_{ext} = 0$).[150,158] Here, if $f_{ext} = 0$, the efficiency is zero.

The *Stokes efficiency* (η_{Stokes}) is distinct from the free-energetic efficiency, instead defined to include work against viscous friction even in the absence of an external conservative force:[153]

$$\eta_{Stokes} = \frac{\zeta \langle v \rangle^2}{J\Delta\mu + f_{ext}\langle v \rangle} \tag{16}$$

where ζ is the Stokes drag coefficient of the motor and cargo. η_{Stokes} remains positive for $f_{ext} = 0$. Evaluating the Stokes efficiency allows performance comparisons between machines when the input free energy is not converted to free energy output.

The thermodynamic uncertainty relation (eq 28)[131] limits the achievable molecular machine free-energetic efficiency[159] for a given pulling speed and conservative force:

$$\eta \le \frac{1}{1 + \frac{v k_B T}{D f_{ext}}} \tag{17}$$

where D is the motor diffusivity under nonequilibrium driving.[f] The Stokes efficiency is similarly bounded:[159]

$$\eta_{Stokes} \le \beta\zeta D \tag{18}$$

Equations 15−18 describe the efficiency of translational motors, but analogous expressions can be developed for other molecular machine types.

With multiple molecular machines, the efficiency can be enhanced as a result of the many-body effects of machine interactions.[160,161]

Living things cannot avoid spending free energy to drive molecular machines. However, resource limitations incentivize biology to reduce the free energy consumed by a particular task (all else being equal), so it is perhaps unsurprising that molecular machines can achieve remarkable efficiencies. F_OF_1-ATP synthase has a (free-energetic) efficiency of ∼90% in animal mitochondria and ∼65% in chloroplasts.[162] Although kinesin has tightly coupled ATP hydrolysis and forward steps,[52,53,163] much of the free energy kinesin consumes from ATP hydrolysis is dissipated, and its efficiency is far from unity.[101]

6.2. Flux and Output Power

The flux J measures the average machine progress, or the rate at which cycles are completed. The output power $\mathcal{P}$ is the rate at which a machine performs useful work and is proportional to the flux:

$$\mathcal{P} = J\Delta w \tag{19}$$

where Δw is the work per machine cycle. As either J or Δw is independently increased, the power increases proportionally. However, the flux itself is often a (typically decreasing) function of Δw. As Δw approaches (from below) the affinity ω_{tot} per cycle in the absence of a load, the flux approaches zero.[150,164] When Δw reaches ω_{tot}, the flux goes to zero (see section 6.4).

Molecular machines can achieve rapid throughput. A bacterial flagellum typically rotates at ∼100 turns/s[165] but can reach angular frequencies of ∼300 turns/s,[166] as can F_OF_1-ATP synthase[167] (exceeding jet-engine turbines).[103] Conventional kinesin translates at 800 nm/s in vitro (100 steps/s) and 2000 nm/s in vivo.[25] Myosin XI can reach 7 μm/s.[168]

Flux is important because biomolecular machines must outpace entropy increases due to the second law of thermodynamics and act as essential players in the competition with other organisms. Evidence is accumulating that biological evolution values molecular machine flux for DNA replication and tRNA selection during translation,[169] during the thermoadaptation of enzymes,[170] in the optimization of enzymes to operate near the diffusion limit,[171] and in bacterial adaptation machinery to sense external concentrations.[172] In addition to allowing organisms to increase the rate of biochemically driven processes, fast molecular machines can conserve resources by requiring fewer machines to complete an equivalent task.

Free energy must be spent to drive directed behavior of molecular machines. While increasing free energy consumption can increase the machine flux, the way in which the free energy is spent can also be adjusted to increase the machine flux. Here we examine how to improve the transduction of free energy into rapid directed motion.

Molecular machine flux is related to the driving strength. For a single-state unicyclic machine, the forward and reverse transition rate constants are related by $k^+/k^- = e^{\beta\omega_{tot}}$. If the effect of dissipation is solely to enhance the forward rate, then the flux is $J = k^0(e^{\beta\omega_{tot}} - 1)$ for the bare rate constant k^0, giving asymptotic scaling $J \sim e^{\beta\omega_{tot}}$ for $\beta\omega_{tot} \gg 1$ and $J \sim \omega_{tot}$ for $\beta\omega_{tot} \ll 1$.

For a two-stage unicyclic machine,

DOI: 10.1021/acs.chemrev.9b00254
Chem. Rev. 2020, 120, 434−459

$$J = \frac{k_{12}^0 k_{21}^0 (e^{\beta\omega_{tot}} - 1)}{k_{12}^0 e^{\beta\omega_{12}} + k_{12}^0 + k_{21}^0 e^{\beta\omega_{21}} + k_{21}^0} \quad (20)$$

using eq 7 with $k_{ij}^+ = k_{ij}^0 e^{\beta\omega_{ij}}$, $k_{ij}^- = k_{ij}^0$, and $\omega_{tot} = \omega_{12} + \omega_{21}$. Although no longer straightforward, the flux depends on ω_{tot}, as is the case for machines with more stages or multiple cycles. Experiments have confirmed the sensitivity of the molecular machine flux to the affinity, specifically the dependence of the kinesin flux on the ATP concentration.[173,174]

Wagoner and Dill[136] considered a molecular motor with a single-stage cycle and multiple distinct pathways for motor stepping. Their model included a splitting factor $\delta \in [0,1]$ (see section 5.7) that divided the influence of the load Δw (i.e., the work done per machine cycle) into the forward and reverse transition rate constants:

$$k^+ = k^0 e^{\beta\Delta\mu - \beta\delta\Delta w} \quad \text{and} \quad k^- = k^0 e^{\beta(1-\delta)\Delta w} \quad (21)$$

In eq 21, the dissipation $\beta\Delta\mu$ driving forward progress affects only the forward rate constant k^+ and does not change the reverse rate constant k^-. The influence of dissipation can generally be split among the forward and reverse rate constants,[137] as described by eq 11, but for simplicity the dissipation is often assigned to only increase the forward rate constants.

In contrast, in eq 21 the influence of the load Δw is split between the forward and reverse rate constants. For $\delta = 0$, the load only increases the reverse rate constant k^- and leaves the forward rate constant k^+ unchanged, while for the opposite extreme ($\delta = 1$) the load only decreases k^+ and leaves k^- unchanged. The value $\delta = 0$ was found to maximize the motor flux regardless of other details—for optimization of the flux, it is better to accelerate reverse transitions than slow forward transitions. Figure 8 shows that at zero load ($\Delta w = 0$) or stalling load ($\Delta w = \Delta\mu$), the flux is independent of δ; however, at intermediate loads a $\delta = 0$ motor (where the load speeds up reverse transitions) can have many times the flux of a $\delta = 1$ motor (where the load slows down forward transitions). Thus, the distribution of a load shared between slowing down a forward rate and speeding up a reverse rate can substantially influence the overall motor flux.

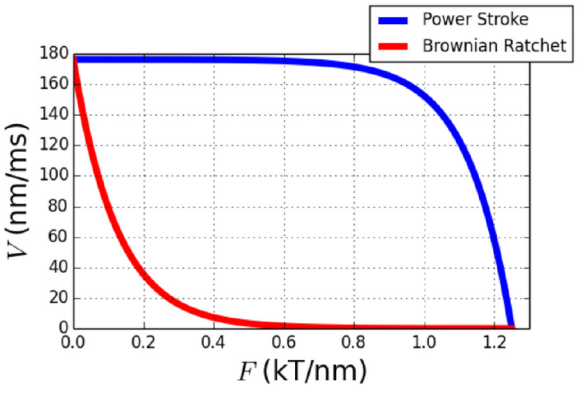

Figure 8. Dependence of the flux on the load distribution. $F \equiv \Delta w/d$ is the resisting force on a motor, and V is the velocity. Under intermediate loads ($0 < F < \Delta\mu/d$), a power stroke (corresponding to $\delta = 0$) maintains a substantially larger velocity than a Brownian ratchet ($\delta = 1$). Here, $d = 8$ nm and $\Delta\mu = 10k_BT$. Reproduced from ref 136. Copyright 2016 American Chemical Society.

The model in eq 21 is for a single-stage machine cycle. Also, as mentioned above, eq 21 splits the impact of the load Δw between the forward and reverse rate constants but models the dissipation $\beta\Delta\mu$ as only increasing the forward rate constant k^+ while leaving the reverse rate constant k^- unchanged. Further work extended the model in eq 21 to cycles with multiple stages and to allow splitting factors to apply to all of the free energy terms, not just those associated with the load.[137] For this more general scenario with multiple stages and splitting of all free energy terms between the forward and reverse rate constants, there is no general optimal splitting factor δ that maximizes the flux for all models. Instead, the optimal δ value depends on specific details of the given molecular machine cycle. The result obtained by Wagoner and Dill is a specific relevant case within the more general model.

Similar to the impact of dividing the free energy between the forward and reverse transitions is the effect of allocating the dissipation across different stages in a multistage molecular machine cycle. The flux-maximizing allocation of free energy to the various transitions is generally uneven.[175] For a two-state cycle, it is

$$\omega_{12}^* = \frac{1}{2}\omega_{tot} + \frac{1}{2}k_BT \ln \frac{k_{21}^0}{k_{12}^0} \quad (22)$$

where ω_{tot} is the affinity for the entire cycle and k_{ij}^0 is the bare rate constant for the $i \rightarrow j$ transition. The flux-maximizing dissipation allocation depends on the bare rate constants k_{ij}^0, which describe the inherent time scales of the individual transitions in the absence of nonequilibrium driving, combining barrier height and diffusivity along the free energy landscape. For the model leading to eq 22, the maximal flux is achieved by allocating more dissipation to accelerate the transitions that are slower at equilibrium, essentially using nonequilibrium driving to compensate for slow equilibrium kinetics. In the limit of large dissipation (where the reverse rates are negligible), this is equivalent to equalizing the forward rates. The flux can depend sensitively on the dissipation allocation, decreasing by orders of magnitude only a few k_BT away from the optimal dissipation allocation.[175] The maximum flux is

$$J^* = \frac{k_{12}^0 k_{21}^0 (e^{\beta\omega_{tot}} - 1)}{k_{12}^0 + k_{21}^0 + \sqrt{k_{12}^0 k_{21}^0}\, e^{\beta\omega_{tot}/2}} \quad (23)$$

Figure 9 shows two-state models for several machines parametrized from experimental data. The dissipations fit to experiment are well-described by uneven allocation (eq 22), while in three cases even allocations are clearly inconsistent with the experimental fits.

Anandakrishnan et al.[177] explored free energy use by a molecular machine that requires several unfavorable transitions. This scenario is inspired by the operation of ATP synthase, which over one rotation binds three ADP molecules and releases them as three ATP molecules. The process of catalyzing each ADP → ATP reaction requires the binding (and hence the driving force) of three protons, involving both a free energy increase (upon binding of a proton) and a later free energy decrease (upon release of a proton), raising the question of how these free energy increases and decreases should be ordered to maximize the ATP synthase flux (Figure 10). Mechanistically, it may seem simpler for a machine like ATP synthase to bind three protons, phosphorylate ADP to

DOI: 10.1021/acs.chemrev.9b00254
Chem. Rev. 2020, 120, 434−459

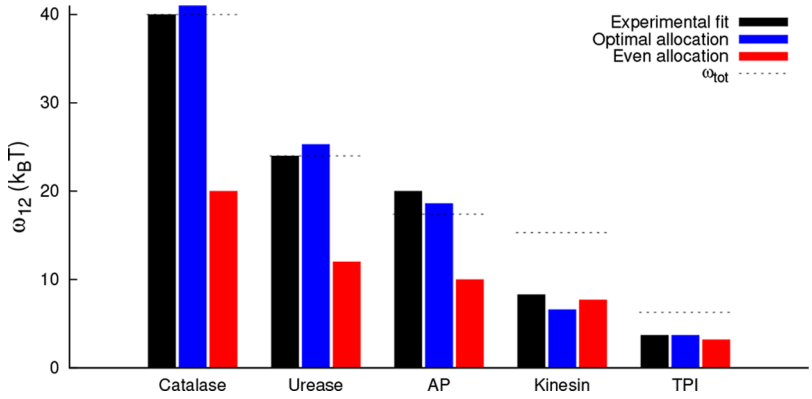

Figure 9. Maximum flux predictions for dissipation allocation. For several enzymes, comparisons of the dissipation allocation obtained from a fit to experimental data (black), the allocation that maximizes the flux from eq 22 (blue), and even allocation (red) are shown. Here ω_{12} is the larger dissipation in a two-state discrete model, and $\omega_{tot} = \omega_{12} + \omega_{21}$. Experimental fits are from Hwang and Hyeon.[176] AP, alkaline phosphatase; TPI, triose phosphate isomerase. Adapted from ref 175.

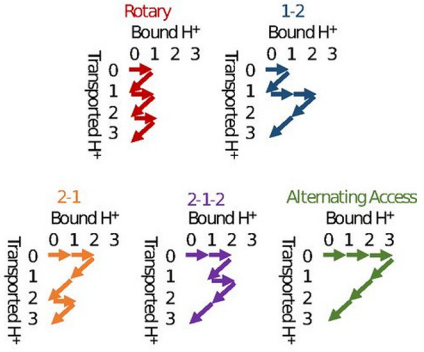

Figure 10. Various schemes for the proton-transport order of ATP-synthase-like enzymes. Possible mechanisms for ATP-synthase-like enzymes based on different proton-transport orders for a 3:1 H^+:ATP stoichiometry are shown ("Rotary" labels the actual mechanism). Addition and removal of bound H^+ correspond to increases and decreases in free energy, respectively. Adapted from ref 177.

ATP, and release ATP and the three protons. Anandakrishnan et al. found that simultaneously processing three ATPs and sequentially binding and releasing individual protons (corresponding to repeated but modest free energy increases followed by decreases) results in a faster cycle than all of the alternative reaction schemes. The rotary mechanism of ATP synthase allows this repetitive cycle, avoiding unnecessarily high free energy increases that would decrease the cycle flux by dividing what could be a single high free energy barrier into several lower barriers.

Wagoner and Dill[178] more recently further explored how characteristics of free energy use control the molecular machine flux, bringing existing and new results into a single framework. They found that equal barrier heights maximize the flux, consistent with earlier work.[175] Using free energy from fuel to cancel out free energy costs of mechanical work also leads to higher flux, similar to aligning multiple free energy components such that together they are optimal.[137] For a wider range of models, they showed that an early transition state ($\delta = 0$) increases the machine flux. Echoing the results of Anandakrishnan et al.[177] for ATP synthase, Wagoner and Dill found that higher flux is achieved by splitting up the cost of external work across many stages.

Overall, recent work has shown that the details of a free energy landscape (dissipation allocation, ordering of increases/decreases, and splitting of free energy for each transition) can be adjusted to speed up molecular machine operation, even if the affinity (i.e., the free energy budget) remains unchanged. It is important to note that the optimal free energy landscape depends on the applied constraints, so there is no universally optimal choice.[137,175]

6.3. Precision

The stochastic nature of molecular machine operation inextricably produces substantial variation in the behavior of an individual machine. The precision of an individual machine's motion is commonly defined in terms of the *Fano factor* (F, defined as the ratio between the variance and mean of a stochastic quantity[179]) of the number (n) of machine cycles completed:

$$F \equiv \frac{\langle n^2 \rangle - \langle n \rangle^2}{\langle n \rangle} \tag{24}$$

For a transport motor such as kinesin, n is the net number of forward steps taken.[g]

For a transport motor taking steps of size d, the average progress is the average distance $\langle X \rangle = d\langle n \rangle$, and the Fano factor is

$$F = \frac{\langle X^2 \rangle - \langle X \rangle^2}{d\langle X \rangle} \tag{25}$$

Substituting the diffusivity $D \equiv (\langle X^2 \rangle - \langle X \rangle^2)/(2t)$ and mean velocity $v \equiv \langle X \rangle / t$ reformulates the Fano factor as the *randomness parameter* (r):[173,182]

$$r \equiv \frac{2D}{vd} \tag{26}$$

Machines with small step-number Fano factors or randomness parameters have more reliable behavior and are generally considered to be higher-performing. The randomness parameter has been directly measured to be $0.3 \lesssim r \lesssim 1.5$ in kinesin experiments across a wide range of forces and ATP concentrations.[52,183,184]

For a general unicyclic motor with N states, the Fano factor has a lower bound:[185,186]

$$F \geq \frac{1}{N} \tag{27}$$

DOI: 10.1021/acs.chemrev.9b00254
Chem. Rev. 2020, 120, 434−459

Motors with more states per cycle can achieve greater precision, provided that the transitions have similar rate constants.[182] Equation 27 has been used to estimate the numbers of states in the cycles of biomolecular motors.[184]

Barato and Seifert derived a tighter limit on motor precision that also incorporates free energy consumption.[131] For a single-stage (i.e., one-state) motor with forward rate constant k^+ and reverse rate constant k^-, the mean net number of forward transitions or steps is $\langle n\rangle = (k^+ - k^-)t$, and the variance is $\langle n^2\rangle - \langle n\rangle^2 = (k^+ + k^-)t$. The rate constant ratio is related to the affinity as $k^+/k^- = \exp[\beta\omega_{tot}]$ (a special case of eq 11). Thus, the dissipation rate is $\Omega = \omega_{tot}\langle n\rangle/t = (k^+ - k^-)\omega_{tot}$. Combining the dissipation rate with the uncertainty $\epsilon^2 \equiv (\langle n^2\rangle - \langle n\rangle^2)/\langle n\rangle^2 = (k^+ + k^-)/[(k^+ - k^-)^2 t]$ yields the *thermodynamic uncertainty relation*

$$\Omega t\epsilon^2 = \omega_{tot}\coth\frac{1}{2}\beta\omega_{tot} \geq 2k_BT \tag{28}$$

Equation 28 relates the affinity ω_{tot} to the achievable uncertainty ϵ^2. For example, a precision of 1%, or $\epsilon^2 = 10^{-4}$, requires $\omega_{tot} \geq 2 \times 10^4 k_BT$.

For an N-state motor cycle, Barato and Seifert additionally showed that the precision of motor progress is limited by[187]

$$\frac{\langle n^2\rangle - \langle n\rangle^2}{\langle n\rangle} \geq \frac{1}{N}\coth\frac{\beta\omega_{tot}}{2N} \geq \frac{1}{N} \tag{29}$$

Equation 29 generalizes eq 27 to finite dissipation, as eq 27 is the $\omega_{tot} \to \infty$ limit of eq 29. Equation 29 quantifies the greater precision that autonomous motors can achieve with a larger number N of discrete states per cycle and/or larger affinity ω_{tot}.

Barato and Seifert initially proved eq 28 for unicyclic networks and conjectured that it would hold more generally;[131,187] their conjecture was soon proved by Gingrich et al. using large deviation theory.[188] The thermodynamic uncertainty relation (eq 28) has been generalized to finite times[189,190] and discrete time,[191] and the bound can tighten for special cases.[192] Conversely, simply adding a large (and hence slowly diffusing) towed cargo to a molecular motor[193−195] can considerably increase the achievable precision because the effective number, N, of motor states is sensitive to strong coupling of the motor to its surroundings.[196]

The thermodynamic uncertainty relation can be applied widely, constraining heat engines in addition to isothermal motors,[197] and can be used to constrain other performance metrics, such as the efficiency of a molecular motor pulling against a constant force.[159] Beyond motors and machines, the thermodynamic uncertainty relation has been used to constrain molecular copying[198] and self-assembly processes.[199]

Assessment of several cases has shown that biomolecular motor operation approaches the thermodynamic uncertainty relation limit.[200] Equality on the righthand side of eq 28 can be achieved by a process with a Gaussian distribution of dissipation arbitrarily far from equilibrium.[201]

6.4. Stall Force

Molecular motors can work against both conservative external forces and viscous forces that oppose the motion of the motors themselves or their towed cargo.[202] When the forces opposing a motor reach the *stall force*, the mean motor velocity drops to zero. Machines with higher stall forces are able to make forward progress under a broader range of conditions.

The stall force is limited by the free energy available per motor cycle with zero load[203] (i.e., the affinity ω_{tot} at zero load) and the motor step size d:[164]

$$f_{stall} \leq \frac{\omega_{tot}}{d} \tag{30}$$

Equality in eq 30 corresponds to a *tightly coupled* motor, where consumption of each unit of fuel leads to a forward step.[38] In contrast, a *loosely coupled* motor has back steps that consume free energy or futile cycles in which free energy is consumed but no steps are taken, thereby decreasing the stall force.[38]

Of course, higher ω_{tot} produces a higher stall force. Less obviously, longer individual steps d lead to a lower stall force for a given affinity.

Kinesin takes 8 nm steps and stalls at ∼4 pN (in the presence of 2 mM ATP),[60] compared with myosin V, which takes 36 nm steps and stalls at 1.6 pN (in the presence of 2 mM ATP),[204] and dynein, which takes 8 nm steps and stalls at anywhere from 1 to 7 pN depending on the species.[205] RNA polymerase can achieve a stall force as high as 30 pN.[206]

6.5. Processivity

Molecular motors can take many consecutive steps along their intracellular filament tracks before eventually detaching. The number of such steps taken before detachment is a stochastic quantity, with the typical number defining the *processivity*. As the primary role of many of these molecular motors is to transport cargo along filaments, more processive motors (i.e., motors that take more steps before detachment) are considered to have better performance.

Transport motors can achieve impressive processivities. For example, conventional kinesin typically takes ∼100 steps before detaching.[52] Myosin V has a characteristic run length of ∼1400 nm (corresponding to ∼40 steps of 36 nm) under a small load.[207]

6.6. Specificity

Certain biomolecular machines copy a sequence of chemical letters or transcribe/translate one sequence type into another: DNA polymerase copies a DNA sequence; RNA polymerase transcribes the DNA sequence into an mRNA sequence; and ribosomes translate a sequence of RNA codons (groups of three nucleotides) into the corresponding sequence of amino acids. These machines have "soft" parts and thus must rely on small energy differences, comparable to k_BT, to discriminate between correct and incorrect copies. This contrasts notably with macroscopic machines, which can be designed with macroscopic energy penalties that are prohibitively large (e.g., a component that does not fit). Thus, these (microscopic) biomolecular copying and translation processes have a nonzero error rate.

Despite these features, molecular machines can achieve low error rates (high *specificities*), as quantified by the fraction of letters in the product that incorrectly represent the initial template.[208] The error rates for DNA replication, RNA transcription, and protein translation have been measured as 10^{-10}−10^{-8}, 10^{-5}−10^{-4}, and 10^{-4}−10^{-3}, respectively.[169]

6.7. Performance Trade-Offs

Variation of operational parameters can alter these measures of performance. One might imagine that optimizing various measures of performance would lead to ideal molecular machine operation; however, a given molecular machine

DOI: 10.1021/acs.chemrev.9b00254
Chem. Rev. 2020, 120, 434−459

design cannot simultaneously optimize all measures of performance.

The Pareto frontier[209,210] (Figure 11) is defined by the set of points in the space of performance measures for which improving one performance measure requires degrading other distinct measures, leading to trade-offs between them. Essentially, the Pareto frontier constitutes the set of achievable combinations of performance on various measures such that there is no unambiguously better achievable combination.

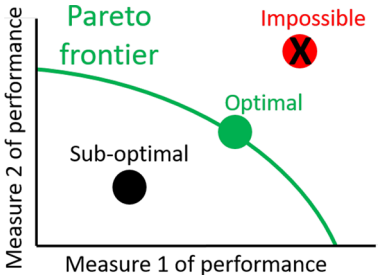

Figure 11. The Pareto frontier represents a range of possibilities for optimal performance given the unavoidable trade-offs between distinct measures of performance. Points not on the Pareto frontier (e.g., labeled "Sub-optimal") are worse on at least one performance measure than a point on the Pareto frontier (e.g., labeled "Optimal"), and no better at any other tasks. Points beyond the Pareto frontier (e.g., labeled "Impossible") are not achievable.

Multiobjective optimization, where the relative importance of different performance measures is varied, can be used to identify the Pareto frontier. The frontier can be nonconvex, implying a phase transition (rather than a continuous crossover) in the optimal strategy as the relative importances are varied.[211]

In the sections above, we have already outlined some trade-offs. As the focus of this review is on how dissipation relates to molecular machine operation, these trade-offs include flux versus dissipation (eq 23), precision versus dissipation (eqs 28 and 29), and stall force versus dissipation (eq 30).

Here we discuss trade-offs between dissipation and specificity of copying/transcribing sequences of DNA/RNA nucleotides (letters); similar principles apply to amino acids and translation. The copying enzyme has "right" (R) and "wrong" (W) substrates competing to be added as the next letter in the sequence (Figure 12). The enzyme goes through intermediate stages before permanently incorporating R into the right product P_R or W into the wrong product P_W. For a wrong substrate with an energy penalty Δ relative to the right substrate, an equilibrium process has an error rate $e^{-\beta\Delta}$. However, this copying process is driven out of equilibrium by free energy consumption to cyclically sample many possible right and wrong substrates (represented by cycles in Figure 12), which can decrease the error rate to a minimum bound of $e^{-2\beta\Delta}$.[212−214] This relationship represents a trade-off between specificity and free energy consumption, and decreasing the error rate from the equilibrium value to the nonequilibrium value depends on the free energy used per cycle to drive the process out of equilibrium.

For given energy differences and nonequilibrium driving, there is also a trade-off between copying speed and specificity. Lower error rates come at the cost of many sampling cycles, decreasing the copying speed. Recent work explored this trade-off and found that DNA copying and protein translation are near the Pareto frontier for speed and specificity.[169] That work also found that DNA copying and protein translation in vivo appear to favor speed over specificity once a certain level of specificity is reached.

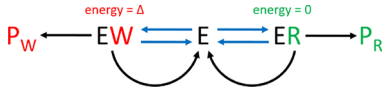

Figure 12. Simplified kinetic proofreading scheme similar to those in DNA replication, RNA transcription, tRNA aminoacylation (charging), and protein translation. Straight blue arrows in two directions represent reversible binding of the right substrate (R, green) or the wrong substrate (W, red) to a copying enzyme (E), and straight black arrows denote the permanent incorporation of the substrate into the copying product (P). Curved black arrows represent cyclic sampling of many candidate substrates for the copy, driven by the dissipation of free energy. The two arrow types from ER and EW to E represent distinct physical processes: the straight blue arrows represent reversal of the binding process, while the curved black arrows represent the removal of R and W using free energy dissipation and are not simple reversals of the respective binding processes. Combined with the energy penalty Δ for wrong substrates, cyclic sampling substantially decreases the probability of selecting the wrong substrate.

Beyond even a broad definition of molecular machines, other processes such as T-cell activation,[215,216] bacterial chemotaxis,[172,217] and signal transduction[218] also demonstrate trade-offs among energy, speed, and accuracy.

7. EXTERNAL DRIVING COSTS

Free energy transduction requires the input of free energy. A common framework is to guide the machine by varying a control parameter (see section 5.4), driving the machine between distinct macrostates, and imparting energy to the machine. Such externally imposed control of a molecular machine comes at the thermodynamic cost of dissipated energy that is no longer available to perform work. Given the tasks, models, and physical principles underlying molecular machine operation described above, we now examine the energy cost for deterministically driven molecular machine dynamics.

In single-molecule experiments, such explicitly time-dependent driving can be imposed externally by an experimentalist; in vivo operation of autonomous molecular machines is not subject to such externally imposed dynamical protocols. Rather, such driving can come from another mechanically coupled molecular component, often another machine or another part of the given machine (e.g., in ATP synthase, F_O mechanically rotates the central crankshaft to drive F_1). In this sense, an upstream machine component can mimic the nonequilibrium variation provided by an experimentalist.

7.1. Directional Differences

Directed behavior of molecular machines can derive from asymmetric responses to external perturbations.[17] The distinctiveness of the system response can be quantified by the time asymmetry A, which quantifies the ease of distinguishing between the forward and reverse trajectory distributions for an externally driven process. This can be expressed information-theoretically as the Jensen−Shannon divergence (JS) of the forward and reverse trajectory distributions:[219]

$$A[\Lambda] \equiv \mathrm{JS}(P[x|\Lambda],\, \tilde{P}[\tilde{x}|\tilde{\Lambda}]) \tag{31}$$

where

DOI: 10.1021/acs.chemrev.9b00254
Chem. Rev. 2020, 120, 434−459

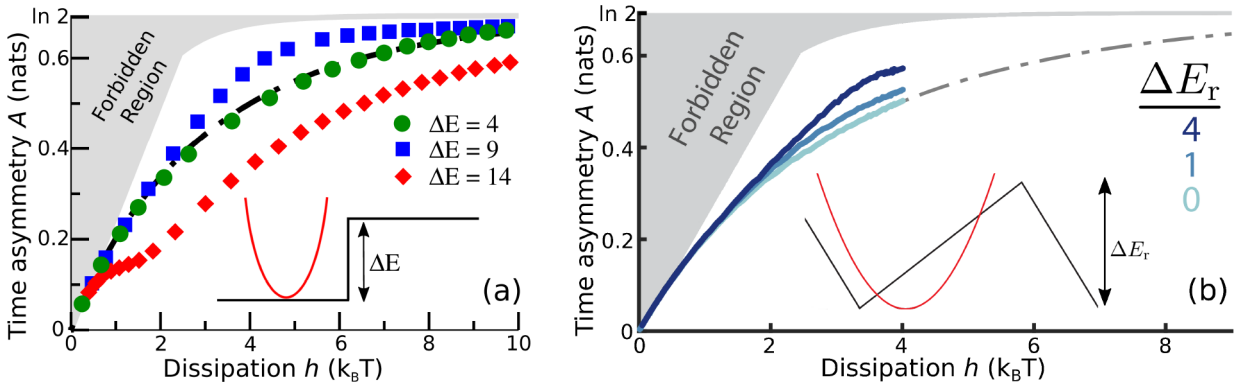

Figure 13. Time asymmetry A vs hysteretic dissipation h. (a) Green circles, blue squares, and red diamonds: parametric plots when driving a system up a step potential for low, intermediate, and high steps, respectively. (b) Light-, medium-, and dark-blue points: parametric plots for driving a system across a sawtooth for negligible, low, and higher sawteeth, respectively. Different points for each color represent different driving speeds, with higher time asymmetry A and dissipation h from faster driving. The dot-dashed black curves show linear response, and the gray regions indicate unfeasible time asymmetries for a given dissipation. Adapted with permission from (a) ref 226 and (b) ref 227. Copyright 2016 and 2019 American Physical Society, respectively.

$$\mathrm{JS}(p, q) \equiv \frac{1}{2}\sum_i \left[p_i \ln \frac{p_i}{\frac{1}{2}(p_i + q_i)} + q_i \ln \frac{q_i}{\frac{1}{2}(p_i + q_i)} \right] \tag{32}$$

is a measure of the distance between two probability distributions p and q.[220] Here $P[x|\Lambda]$ is the probability of forward trajectory x during the forward protocol Λ and $\tilde{x}$ and $\tilde{\Lambda}$ are the time reversals of trajectory x and protocol Λ, respectively, such that $\tilde{P}[\tilde{x}|\tilde{\Lambda}]$ is the probability of a reversed trajectory when the protocol is run backward. The time asymmetry A represents the expected distinguishability of system trajectories driven by the forward protocol Λ compared with those driven by its time-reversed counterpart $\tilde{\Lambda}$.

The Jensen–Shannon divergence contains two Kullback–Leibler divergences,

$$D(p, q) \equiv \sum_i p_i \ln \frac{p_i}{q_i} \tag{33}$$

which have also been used to quantify irreversibility.[221,222] In contrast to the Kullback–Leibler divergence, the Jensen–Shannon divergence is symmetric with respect to the two input probability distributions, such that switching the "forward" and "reverse" assignments does not change its value.

By the use of the Crooks fluctuation theorem (eq 13), the Jensen–Shannon divergence of the trajectory distributions (eq 31) can be rewritten[223] in terms of work distributions from driving in both directions:[219]

$$A[\Lambda] = \frac{1}{2}\left\langle \ln \frac{2}{1 + \exp(-\beta W[x|\Lambda] + \beta\Delta F)} \right\rangle_{\Lambda} + \frac{1}{2}\left\langle \ln \frac{2}{1 + \exp(-\beta W[\tilde{x}|\tilde{\Lambda}] - \beta\Delta F)} \right\rangle_{\tilde{\Lambda}} \tag{34}$$

where $W[x|\Lambda]$ is the work done over system trajectory x during the forward protocol Λ and ΔF is the equilibrium free energy difference over the forward protocol. This makes time asymmetry experimentally measurable.

A trajectory ensemble under protocol $\tilde{\Lambda}$ that is not the time reversal of the trajectory ensemble under Λ indicates a departure from equilibrium and requires free energy dissipation. This free energy cost is quantified by the hysteretic dissipation,

$$h[\Lambda] \equiv \frac{1}{2}(\beta\langle W[x|\Lambda]\rangle + \beta\langle W[\tilde{x}|\tilde{\Lambda}]\rangle) \tag{35}$$

$h[\Lambda]$ is the average work for the forward and reverse protocols, which is equal to the average excess work because the free energy differences cancel.[219]

Low time asymmetry indicates that a system responds similarly to driving in both directions, while high time asymmetry indicates distinct responses depending on the driving direction. The distinct responses to driving could facilitate the directed dynamics required for molecular machine function, and the time asymmetry generated for a given amount of free energy dissipation assesses how effectively the free energy has been spent for the purpose of generating directed behavior. Accordingly, biological evolution may favor biomolecular machines that achieve a high time asymmetry for a given dissipation cost, motivating investigation of what process characteristics lead to relatively high asymmetry (eq 34) for a given dissipation (eq 35).

Initial empirical investigations, including experiments[219,224] and molecular dynamics simulations,[225] found time asymmetry trade-offs with dissipation that remain near the linear-response prediction.[219] In contrast, when a step-function energy landscape (Figure 13a inset) was used to represent an idealized free energy storage process (with $\Delta F > 0$), intermediate step heights led to time asymmetries that could exceed the linear response for a given dissipation[226] (Figure 13a). Additionally, for a sawtooth energy landscape (Figure 13b inset) with $\Delta F = 0$ (frequently used to represent molecular machines), high and symmetric intervening barriers between consecutive states led to high asymmetry for a relatively low dissipative cost[227] (Figure 13b).

Both step-function and sawtooth energy landscapes allow time asymmetry to exceed linear response, although with distinct strategies—intermediate-height step function contrasting with high sawtooth. In both cases, the system is driven by translation of a quadratic energy trap, with medium-strength traps maximizing the time asymmetry by balancing reliable driving to a given final state (achieved with a narrow trap at high energy cost) against the increased dissipative cost associated with more tightly constraining a system.[226,227]

DOI: 10.1021/acs.chemrev.9b00254
Chem. Rev. 2020, 120, 434–459

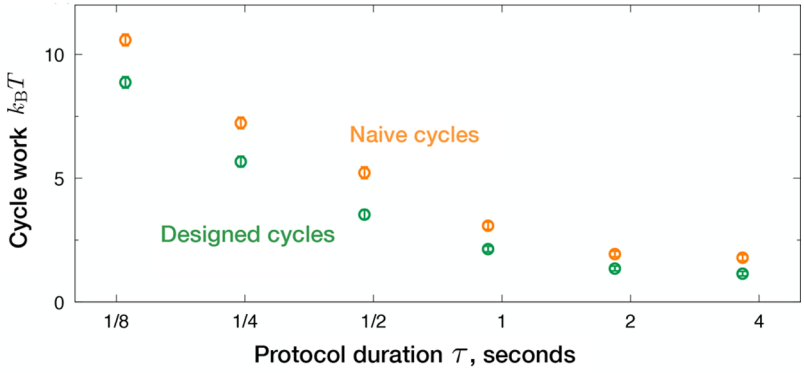

Figure 14. Designed protocols to unfold and refold DNA hairpins systematically require significantly less work than corresponding naive protocols. The mean cycle work $\langle W^{\text{unfolding}} + W^{\text{refolding}} \rangle$ during naive (orange) and designed (green) protocols is shown as a function of protocol duration. Reproduced from ref 229.

Overall, driving a system such that it can transiently "get stuck" can provide distinct forward and reverse trajectory distributions that lead to higher time asymmetries for a given dissipation.[227]

Beyond finite transitions driven by control protocols, the relationship between thermodynamic cost and reliable directed behavior of stochastic processes can be extended to NESS processes. The average entropy production per unit time, $\langle \mathrm{d}S/\mathrm{d}t \rangle$, to generate a NESS with directed behavior in a finite average time $\langle \tau \rangle$ is

$$\frac{1}{k_B}\left\langle \frac{\mathrm{d}S}{\mathrm{d}t} \right\rangle = \frac{L(1-2\alpha)}{\langle \tau \rangle} \tag{36}$$

where L is the threshold amount of progress for directed behavior (how far in the forward or reverse direction the system must progress), and α is the probability that the system will run in the correct direction.[228] Faster processes and those with a higher threshold for sufficient progress have a higher entropy cost per unit time for directed behavior.

7.2. Deterministic Driving

When a control parameter λ changes sufficiently slowly, the system remains near equilibrium and is well-described by linear response theory.[67,147] For a system adhering to linear response, it can be shown that the instantaneous excess power (i.e., the power beyond that required when the system is equilibrated throughout the protocol) required during a control protocol (section 5.4) because the system is out of equilibrium is given by[148]

$$\mathcal{P}_{\text{ex}}(t_0) = \zeta(\lambda(t_0)) \cdot \left(\frac{\mathrm{d}\lambda}{\mathrm{d}t}\right)^2_{t=t_0} \tag{37}$$

where ζ is a generalized friction coefficient that governs the near-equilibrium response and represents the energetic cost of changing the control parameter sufficiently fast to drive the system out of equilibrium:

$$\zeta(\lambda(t_0)) \equiv \beta \int_0^\infty \langle \delta f(0) \delta f(t) \rangle_{\lambda(t_0)} \, \mathrm{d}t \tag{38}$$

Here $\delta f \equiv f - \langle f \rangle_{\lambda(t_0)}$ is the deviation of the conjugate force f from its equilibrium average $\langle f \rangle_{\lambda(t_0)}$ at a fixed control parameter value $\lambda(t_0)$. For instance, when the control parameter is the separation between two optical traps,[229] the conjugate force is the tensile force with which the biomolecule resists further extension. $\langle \delta f(0) \delta f(t) \rangle_{\lambda(t_0)}$ is an autocorrelation function: at $t = 0$ it equals the force variance $\langle \delta f^2 \rangle_{\lambda(t_0)}$, while for $t > 0$ it represents how quickly the system forgets its initial condition. The generalized friction $\zeta(\lambda)$ can be decomposed into the product of the force variance and the integral relaxation time $\tau(\lambda) \equiv \int_0^\infty \frac{\langle \delta f(0) \delta f(t) \rangle_\lambda}{\langle \delta f^2 \rangle_\lambda} \, \mathrm{d}t$, which is the characteristic lifetime of force fluctuations.

Equation 38 is an example of a fluctuation−dissipation theorem relating equilibrium fluctuations to dissipation out of equilibrium. In particular, ζ is a Green−Kubo coefficient[230] expressing a transport coefficient as a temporal integral of a correlation function, in this case the generalized friction coefficient in the space of control parameters as an integral of the force autocorrelation function.

How do we minimize the excess work (i.e., the time integral of eq 37 over a control protocol of fixed duration) to waste as little energy as possible? In general, proceeding slowly reduces the excess work, such that in the quasistatic limit the excess work is zero and the work is equal to the equilibrium free energy difference. Equation 37 expresses the rate of accumulation of excess work along a control protocol. For protocols that minimize work in a fixed duration, the excess power is constant, which is achieved when the control parameter is varied according to[148]

$$\frac{\mathrm{d}\lambda^{\text{opt}}}{\mathrm{d}t} \propto \frac{1}{\sqrt{\zeta(\lambda(t))}} \tag{39}$$

Implementation of this theory depends only on being able to measure at fixed control parameter the fluctuations of the force conjugate to the control parameter. This gives a phenomenological procedure that does not rely on detailed knowledge of either the kinetics or thermodynamics of the system. (If one does have such detailed knowledge, then protocols that minimize work far from equilibrium can be found.[231−233])

Several groups have used this framework to examine optimal protocols in model systems.[148,234−240] Applying this theory to bistable systems representing thermally activated processes[241] leads to the intuition that energetically efficient control requires relatively slow perturbation when the system is on the verge of a major transition, essentially letting random thermal fluctuations kick the system over a given barrier "for free" without energy input from the controller. Other extensions have generalized this control framework to

DOI: 10.1021/acs.chemrev.9b00254
Chem. Rev. 2020, 120, 434−459

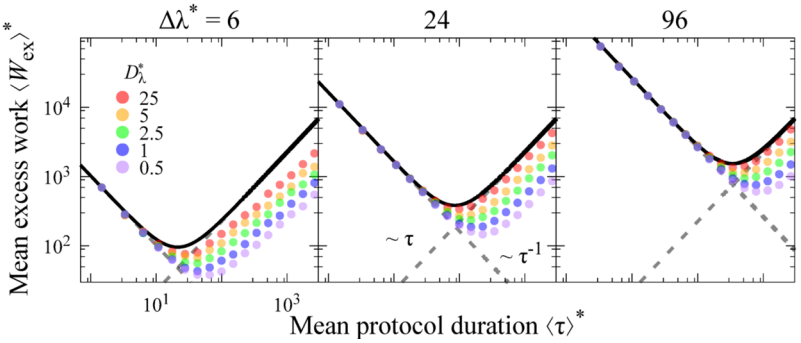

Figure 15. Excess work for a stochastic protocol is minimized at finite protocol duration. The mean dimensionless excess work, $\langle W_{ex}\rangle^* \equiv \beta\langle W_{ex}\rangle$, is shown as a function of mean protocol duration, $\langle\tau\rangle^* \equiv \tau/(2\beta Dk)^{-1}$ (where k is the harmonic trap spring constant). For underdamped control parameter dynamics and large dimensionless protocol distances $\Delta\lambda^* \equiv \Delta\lambda/(\beta k)^{-1}$, where the control parameter dynamics is locally deterministic, numerical simulations (circles) agree with the linear-response approximation (solid black curve), equal to the sum of terms proportional and inversely proportional to the protocol duration (dashed gray curves). The dimensionless control parameter diffusion coefficient $D_\lambda^* \equiv D_\lambda/D$ (where D is the system diffusion coefficient) interpolates between overdamped (purple) and underdamped (red) control parameter dynamics. Reproduced with permission from ref 249. Copyright 2018 European Physical Society.

nonequilibrium steady states[242,243] and to models of rotary machines[244] and chemical reaction networks.[245]

Proof-of-principle experiments recently demonstrated the utility of this theory for predicting energy-conserving behavior in nanoscale biophysical systems[229] using a DNA hairpin (a small piece of DNA that spontaneously folds up on itself) as a model system. Measurements of force fluctuations at fixed optical-trap separation showed that the generalized friction is maximized in the "hopping" regime where the DNA hairpin is equally likely to be folded or unfolded. The optical traps were then dynamically modulated to rapidly stretch the ends of the DNA hairpin (putting work into the hairpin and unfolding it) and then bring the hairpin ends close together (allowing the hairpin to refold, thereby recovering work). The energy lost during cycles designed to proceed slowly through the hopping regime was significantly less than the energy lost during naive cycles that proceeded at a constant speed (Figure 14). This energy savings was found systematically at a variety of cycle speeds and for two different hairpins differing dramatically in their relaxation times.

7.3. Stochastic Driving

The theory in section 7.2 focuses on deterministic driving of a system, where a control parameter follows a fixed temporal schedule. Biomolecular machines do not typically experience an experimentalist deterministically changing a control parameter. Instead, they operate autonomously, responding to the stochastic fluctuations of coupled nonequilibrium systems.

For example, in ATP synthase, the F_1 subunit is driven by another subunit, F_O, that itself operates stochastically. Experimental observation of F_1 rotational statistics indicates a small number of metastable angular states separated by energetic barriers.[41] When the angle of a magnetic trap (the control parameter for single-molecule driving of F_1; see section 2.1) is centered at a barrier separating two adjacent metastable states, the equilibrium probability is split equally between the two states, giving the maximal torque variance $\langle\delta f^2\rangle$ and maximal torque relaxation time, hence maximizing their product, the friction coefficient ζ.[244]

Equation 39 provides intuition on how an experimentalist (or F_O in vivo) should drive the rotation to minimize energy expenditure: where the friction coefficient is large—where the system puts up large resistance to rapid control parameter changes, at the rotational energetic barriers—the minimum-dissipation protocol proceeds slowly, giving thermal fluctuations maximal time to kick the system over the barrier "for free".

Since F_O itself is stochastic and hence cannot impose deterministic driving protocols on F_1, it would have to resort to a stochastic mimic of such a designed protocol. In particular, if F_O itself has metastable rotational states that are out of phase with those of F_1, then the stochastic protocol would amount to rapid rotations followed by pauses at rotational states corresponding to the hopping regime, where F_1 at equilibrium is evenly split between two rotational states, thereby forming a near analogue of the designed deterministic protocols discussed above.

Evolved machines provide tantalizing hints of out-of-equilibrium behavior that would reduce energy consumption. For example, the ϕ29 DNA packaging motor slows down (i.e., it packages shorter stretches of DNA with longer intervening pauses) as the ϕ29 viral capsid is increasingly filled.[246,247] This behavior is consistent with predictions of the linear-response control theory, as the relaxation time for the DNA in the capsid increases strongly with packing fraction. Similarly, translating ribosomes appear to "change gear" when they encounter an RNA hairpin that impedes translation: the ribosome slows down while surmounting the energetic barrier represented by the hairpin.[248] Both examples could be interpreted as driving protocols that proceed slower where the friction coefficient is higher and therefore are predicted to reduce dissipation.

Motivated by stochastic mechanical driving in molecular machines, the study of such stochastic protocols—where the control protocol does not evolve deterministically but rather with its own stochastic dynamics—reveals an interesting qualitative feature: stochastic control-parameter fluctuations on average require net work, which continually accumulates along the protocol. Thus, the work due to stochastic fluctuations increases with the protocol duration; since the work due to the mean protocol decreases with duration, the resulting trade-off leads to stochastic protocols that minimize the work at intermediate protocol durations[249] (see Figure 15).

Extension of these ideas to discrete driving protocols (inspired by the effectively instantaneous nature of chemical reactions compared with other relevant time scales) reveals a

DOI: 10.1021/acs.chemrev.9b00254
Chem. Rev. 2020, 120, 434−459

thermodynamic cost that remains even in the quasistatic limit.[250]

Active efforts currently seek to situate the developing framework of stochastic and discrete control parameter protocols within the more fully developed stochastic thermodynamics of chemical reaction networks.[251−253]

7.4. Autonomous Driving

Sections 7.2 and 7.3 focused on the dissipation due to system resistance to deterministic or stochastic control protocols. However, the very implementation of a control parameter whose dynamics breaks detailed balance requires dissipation, independent of the dissipation associated with system resistance to the control protocol. When a single-molecule experimentalist implements control of a molecular machine, this cost of control may not be a limiting factor. However, for autonomous machines, notably in vivo molecular machines, there is a cost associated with implementing particular asymmetric driving dynamics that should be included in any accounting of total dissipative costs.

Recent research[102,254] on these "upstream" thermodynamic costs associated with imposing particular time-asymmetric detailed-balance-breaking protocol ensembles[102,255] has opened new vistas on the physical principles governing autonomous molecular machines driven by stochastic protocols. Current research is examining the connections between these imposition costs and the "downstream" dissipation resulting from system resistance to the stochastic control parameter dynamics.[249] Interesting questions also remain about how such thermodynamic flows within strongly coupled systems relate to work and heat flows between weakly coupled systems and the environment.[254]

8. SYNTHETIC MOLECULAR MACHINES

Although extensive discussion is beyond the scope of this review, many of the ideas we have discussed here are being explored from an engineering perspective in synthetic machines.[256] The development of synthetic molecular machines includes pumps, walkers, transporters, and rotary motors.[257−259] In addition to helping us better understand evolved machines, synthetic machines are of interest in their own right because of technological applications,[260] including in computation and information storage/retrieval (memory),[235] renewable energy (artificial photosynthesis),[261] drug delivery, and other biomedical goals.[262]

Synthetic molecular machines have been built or designed that are driven by light,[263] electricity,[264] cycling of chemical concentrations,[265,266] or consumption of their track,[267,268] among other driving modes.[256] Systems driven by cycling of chemical concentrations will not reach a NESS because of time-varying rate constants, although constant and cyclic driving are equivalent in some other respects.[269] In section 5.6, transitions were described as obeying microscopic reversibility. For some systems driven by light, microscopic reversibility will not be followed, as these transitions are not driven by thermal fluctuations over the energy landscape. Instead, these transitions involving light follow the Einstein relations for absorption and stimulated and spontaneous emission.[270]

Although most synthetic molecular machines are driven in an altogether different manner than biomolecular machines, an autonomous synthetic molecular machine was recently developed that is driven by nonequilibrium chemical concentrations. The machine involves a small ring transported around a cyclic molecular track with a preferential direction.[257] It remains to be seen whether molecular machines that operate similarly to their biomolecular counterparts will gain wider use.

9. EMERGING IDEAS

In this section we outline some emerging concepts in machine transduction.

9.1. Information Machines

In most of this review, we have discussed how free energy is used to drive molecular machine operation. Here we briefly outline an alternative "fuel" for driving molecular machines: information.

The second law of thermodynamics dictates that the entropy of an isolated system remains constant or increases. Therefore, in a container of equilibrated gas, the fast (hot) molecules do not spontaneously segregate to one side with the slow (cold) molecules on the other side. However, if an intelligent agent were able to selectively open and close a door separating the two sides, only allowing slow molecules to leave one side and fast molecules to leave the other side, then the temperature of one compartment would increase while the temperature of the other compartment decreases: heat would flow from lower to higher temperature, thereby decreasing the entropy. This scenario was originally proposed by Maxwell,[271] with the intelligent agent known as "Maxwell's demon".[272,273] Szilard's engine[274] is a similar scenario where knowledge of a gas molecule's location is used to extract work from the thermal bath. If the intelligent agent can operate without free energy consumption, both Maxwell's demon and Szilard's engine appear to violate the second law.

Information has a physical manifestation,[275] famously expressed in Landauer's principle, which says that information erasure has a minimum free energy cost of k_BT ln 2 per bit,[276] which has been confirmed experimentally.[277,278] The intelligent agents of Maxwell's demon and Szilard's engine must pay this information erasure cost, saving the second law.[279]

Molecular machines can make forward progress and do useful work using feedback. One implementation[280,281] involves a staircase of states separated by a constant energy interval (Figure 16). Infinite barriers separate each pair of states from its neighbors on both sides. The system is thus confined to a pair of states, with the forward state at a higher

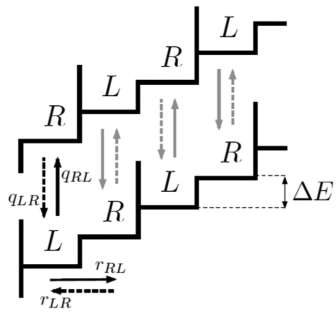

Figure 16. Information motor. A system moves in a periodic potential with two energy levels, with the higher energy level in the direction of desired progress. The potential switches between two configurations, changing which neighboring energy level is accessible from each energy level. If information about the particle location is used to preferentially switch the barriers, the system can progress uphill. Adapted with permission from ref 280. Copyright 2013 American Physical Society.

DOI: 10.1021/acs.chemrev.9b00254
Chem. Rev. 2020, 120, 434−459

energy. The barrier locations can shift to adjust the accessible pair of states depending on the system position. If the system is in the higher-energy of the accessible pair of states when the shift occurs, the previously accessible lower-energy neighboring state is no longer accessible, and instead the system can now access the next higher-energy state up the staircase. If the system is in the lower-energy state when the shift occurs, the previously accessible higher-energy state is no longer accessible, and the system can now access the next lower-energy state down the staircase. If the barriers can be preferentially switched when the system is in the higher-energy state, the system energy increases. Such preferential switching involves feedback and memory, and such information processing has a corresponding free energy cost.[280] Another implementation uses feedback to "push" a particle upstream against flow without doing work.[282]

Including information processing leads to modified forms of the second law[283] that can account for the classic thermodynamic problems of Maxwell's demon and Szilard's engine along with the newer ideas of information machines. In addition to providing a novel driving mode, information machines have distinct thermodynamic behavior, such as linear-response efficiency[284] or free energy dissipation.[280]

9.2. Predictive Machines

Section 7 focused on controlling a machine, rapidly driving it to a new desired macrostate. By contrast, here we take the perspective of the machine, discussing how a system can couple effectively to its environment. Section 6 generally examined machine dynamics that performs well given average nonequilibrium aspects of the environment; here we discuss utilizing fluctuations in a nonequilibrium environment, specifically how properties of a system and its interactions with its environment affect transduction of energetic fluctuations into increased free energy and hence capacity for work.

The difference between the average work $\langle W \rangle$ imparted to the system and the resultant change in the system's capacity for useful work, its nonequilibrium free energy $F_{\text{neq}} \equiv \langle E \rangle - TS$,[285,286] is the dissipated work $W_{\text{diss}} = \langle W \rangle - \Delta F_{\text{neq}}$. (It should be noted that for quasistatic processes—in which environmental changes are sufficiently slow that the system remains at equilibrium throughout—the nonequilibrium free energy reduces to the equilibrium free energy $F_{\text{eq}} = \langle E \rangle_{\text{eq}} - TS_{\text{eq}}$, and the dissipated work vanishes.) The current system state s_t retains information about the current environmental state x_t, as quantified by the mutual information $I_{\text{mem}}(t) \equiv I[s_t; x_t]$.[220] Mutual information I quantifies how much (on average) knowledge of the current system state reduces uncertainty about the current environmental state. Because the system is coupled to its environment and in general an environment does not immediately randomize its state, the current system also has predictive information about the future environmental state x_{t+1}, as quantified by $I_{\text{pred}}(t) \equiv I[s_t; x_{t+1}]$. The work dissipated during environmental dynamics is equal to the difference between these two informations, the unpredictive information (or *nostalgia*) the system retains about the environment, which does not predict the future state of the environment:[287]

$$\beta \langle W_{\text{diss}}[x_t \to x_{t+1}] \rangle = I_{\text{mem}}(t) - I_{\text{pred}}(t) \tag{40}$$

This equivalence of thermodynamic inefficiency $\beta \langle W_{\text{diss}} \rangle$ and predictive inefficiency $I_{\text{mem}} - I_{\text{pred}}$ means that any system, be it an organism, a neuron, or even a single molecular machine, that has been designed, over natural evolution or in a nanoscientist's lab, to be thermodynamically efficient in its interactions with its environment must (at least implicitly) be constructing a parsimonious (not overly complex) model of environmental dynamics.[287,288] At steady state, this nostalgia (for unit-time steps) equals the learning rate, the rate at which a system (because of its own dynamics) increases its mutual information with the environment.[289−293]

Intuitively, this says that thermodynamic efficiency is accomplished by forgetting (i.e., rapidly randomizing and hence relaxing to equilibrium with respect to) degrees of freedom in one's environment that are not predictive of future fluctuations. Possible implications for efficient transduction of environmental fluctuations by molecular machines are that they must ignore the myriad aspects of their environment (e.g., sundry collisions from water molecules) that have no bearing on mechanically meaningful future environmental fluctuations. Conversely, temporal correlations in environmental perturbations can provide thermodynamic advantage if a system can learn them.

9.3. Dissipative Adaptation

This review has emphasized limits and design principles for effective utilization and/or avoidance of dissipation because high-performance molecular machines should be favored by natural selection. Recent research further suggests a relationship between free energy dissipation and the evolution of systems in the absence of natural selection.

England[294] showed within the framework of stochastic thermodynamics[5] that there is a relationship between the degree of irreversibility and the required entropy production for macroscopic transitions:

$$\beta \langle \Delta Q \rangle_{\mathbf{I} \to \mathbf{II}} + \ln \frac{\pi(\mathbf{II} \to \mathbf{I})}{\pi(\mathbf{I} \to \mathbf{II})} + \frac{\Delta S_{\text{int}}}{k_{\text{B}}} = 0 \tag{41}$$

where $\langle \Delta Q \rangle_{\mathbf{I} \to \mathbf{II}}$ is the heat dissipated as the system transitions from state **I** to **II**, $\pi(\mathbf{I} \to \mathbf{II})$ is the probability of a system initially at state **I** transitioning to state **II**, and ΔS_{int} is the entropy change of the system in going from **I** to **II**. However, England also argued that this relationship between irreversibility and entropy production has consequences for self-replicating processes:[294]

$$g_{\max} = \chi e^{\beta \Delta q + \Delta s_{\text{int}}/k_{\text{B}}} \tag{42}$$

in which $g_{\max}$ is the maximum growth rate, χ is the decay rate, and Δq and Δs_{int} are intensive versions of the earlier quantities. Equation 42 argues that the maximum growth rate is limited by the dissipation, durability, and organization: higher dissipation allows higher growth rates, and increased durability and organization decrease the allowed growth rate.

It follows that systems are more likely to follow trajectories that have higher dissipation. Therefore, a system can "adapt" (in the absence of natural selection) to dissipate free energy of the form that is available because those dissipative trajectories are more likely.[295] If a system is self-replicating, this adaptation can be taken further, as systems that follow trajectories allowing improved reception of the provided free energy will have successors that continue to follow more likely trajectories.[296]

DOI: 10.1021/acs.chemrev.9b00254
Chem. Rev. 2020, 120, 434−459

9.4. Enzyme Diffusion Enhancement

Energy can be consumed to create and enhance directed motion, but recent studies have found that energy consumption can also enhance random undirected motion (diffusivity). Essentially, free energy can be transduced into quicker motion or dynamical spreading. Specifically, carrying out catalysis has been found to increase the diffusive mobility of enzymes.[297,298] This diffusion enhancement can be substantial, with the largest observed enhancement being ~80%.[299] This effect increases with higher substrate concentrations and appears to be limited to enzymes performing catalysis, as it is not shared with nearby enzymes.[300] Although higher diffusion occurs at higher temperatures, overall catalytic energy release does not appear to be the cause, as diffusion enhancement has been measured for both endothermic and exothermic reactions.[301] Global energy changes and changes to charge and pH have also been excluded as mechanisms.[302] Enhancement of enzyme diffusion was initially measured with fluorescence correlation spectroscopy (FCS). Recently, the possibility was raised that artifacts in FCS measurements could lead to an apparent increase in measured diffusion without an actual increase in diffusion,[303] but enhanced enzyme diffusion has been confirmed with direct single-molecule imaging.[299]

Efforts to systematically relate enzyme diffusion enhancement to other measurable quantities have met with some success. For some exothermic reactions the diffusivity enhancement is proportional to the catalyzed reaction rate and the heat released by the reaction, with an enzyme-specific proportionality constant.[302] The increased enzyme velocity is thought to be sustained for only a very short period of time, on the order of nanoseconds, following each catalyzed reaction.[302] It has been suggested that enzymes with low proportionality constants between reaction rate and released heat (i.e., enzymes whose diffusion is not significantly enhanced), such as catalase, may be able to achieve higher throughput because the low diffusivity enhancement may indicate relative conformational stability.[302]

There is no consensus for the underlying mechanism driving enhanced enzyme diffusion during catalysis. It has been proposed that the enhanced enzyme diffusivity is due to a "chemoacoustic" effect, where the asymmetric expansion and contraction of the enzyme during and following catalysis generates heat and an asymmetric pressure wave that pushes back on the enzyme to generate the enhanced diffusion.[302] Alternatively, differences in fluctuation ensembles between substrate-bound and -unbound enzyme states could contribute to enhanced diffusivity, particularly for enzymes with low throughput that catalyze endothermic reactions.[301]

Enhanced enzyme diffusion may have biological implications, possibly allowing enzymes to chemotax (move to higher substrate concentrations) and draw together chemically connected enzymes.[300] Beyond just isolated enzymes, a similar effect would reposition the complex of nucleic acid copying enzymes and their template (i.e., DNA/RNA polymerase and DNA) to higher nucleotide concentrations.[297,304] Interestingly, it has also been suggested that enhanced enzyme diffusion could allow enzymes to anti-chemotax (move to lower substrate concentrations), which could smooth out the spatial distribution of enzymatic production.[305]

Recent work has argued that enzyme diffusion enhancement due to catalysis fits within the same framework that describes the diffusion enhancement of traditional motors, such as kinesin, due to dissipation.[176]

10. CONCLUSIONS

By writing that "living matter evades the decay to equilibrium," Schrödinger pointed out the inextricable link between free energy consumption and life.[1] Molecular machines, as pivotal free energy transducers in all living systems, are major participants in this life-sustaining dissipation.

In this review, we have (almost certainly incompletely) summarized recent theoretical efforts in several areas involving free energy transduction by molecular machines. As theorists, we are excited about recent and newly emerging theoretical frameworks to describe and understand molecular machines, and we are continually astounded by and thankful for the ongoing experimental innovation that is absolutely essential for continued advance of this field.

Theory, perhaps especially in biophysics, faces a constant struggle between generalizing to an abstract and all-encompassing framework and meaningfully engaging with a messy and heterogeneous reality. Recognizing this tension, we provisionally suggest a potentially unifying principle that cuts across many molecular machines: effective transduction between different nonequilibrium free energy reservoirs. More broadly, we emphasize the importance of identifying and engaging with a set of stylized facts that together form a consensus description for the operation of many molecular machines.

Nevertheless, despite extensive quantitative characterization of a handful of well-studied model systems, it is important to maintain a sense of humility and avoid overgeneralizing current empirical findings. We thus acknowledge the hubris of attempting to impose conceptual order on a set of systems that have undoubtedly developed in vivo from many diverse evolutionary precursors to serve many diverse functional purposes.

We also caution against overzealous usage of optimization arguments. Even if one can successfully identify measures of performance relevant for natural selection, biomolecular machines may only approach, rather than reach, optimal performance because of genetic drift,[306] finite evolutionary time and path dependence, and shifting situations.

Finally, we beg pardon for possibly excluding or downplaying exciting new research areas and results; any such short shrift likely stemmed not from our judgments of importance but rather from the necessity of concision and our own ignorance.

AUTHOR INFORMATION

Corresponding Authors

*E-mail: aibrown@ucsd.edu.
*E-mail: dsivak@sfu.ca.

ORCID

Aidan I. Brown: 0000-0002-6600-8289
David A. Sivak: 0000-0003-4815-4722

Notes

The authors declare no competing financial interest.

Biographies

Aidan I. Brown is a postdoctoral fellow at the University of California, San Diego. He received his B.Sc. in Physics from the University of

DOI: 10.1021/acs.chemrev.9b00254
Chem. Rev. 2020, 120, 434−459

Guelph and his M.Sc. and Ph.D. in Physics from Dalhousie University. He was a postdoctoral fellow at Simon Fraser University.

David A. Sivak is Assistant Professor of Physics at Simon Fraser University (SFU), an associate member of the SFU Departments of Chemistry and Molecular Biology & Biochemistry, and a Canada Research Chair (Tier II) in Nonequilibrium Statistical Biophysics. He received his A.B. in Applied Mathematics from Harvard University, his B.A. in Philosophy, Politics, and Economics from Lincoln College, University of Oxford, and his Ph.D. in Biophysics from the University of California, Berkeley. He was a Physicist Postdoctoral Fellow at Lawrence Berkeley National Laboratory and an independent Systems Biology Fellow at the University of California, San Francisco. The Sivak group develops nonequilibrium statistical physics and stochastic thermodynamics with applications to biological transduction of free energy and information.

ACKNOWLEDGMENTS

The authors thank Nancy Forde, Chapin Korosec, John Bechhoefer, Steve Large, Miranda Louwerse, Martin Zuckermann, Joseph Lucero, and Emma Lathouwers (SFU Physics), Jason Wagoner (Laufer Center, Stony Brook), and Hong Qian (Washington Applied Math) for insightful and helpful comments on the manuscript. This work was supported by a Natural Sciences and Engineering Research Council of Canada (NSERC) Discovery Grant (D.A.S.) and by a Tier-II Canada Research Chair (D.A.S.).

ADDITIONAL NOTES

[a]Borrowing from economics, a *stylized fact* is a broad generalization that summarizes empirical data but may not capture all cases.[4]

[b]In this review, we use *machine* to describe any free energy transducer but reserve *motor* for machines with a functional translational or rotational motion.

[c]Being out of equilibrium breaks the equilibrium fluctuation−dissipation theorem, but even out of equilibrium, the two behaviors are not unrelated: various nonequilibrium fluctuation−dissipation theorems have been derived, especially in nonequilibrium steady states.[68−70]

[d]There are exceptions, i.e., "one-shot" machines such as the spasmoneme.[78]

[e]It should be noted that some other findings of "reversibility" (e.g., in myosin V[94,95] and kinesin[96]) demonstrated mechanical reversibility without establishing reversibility of the chemical reactions.

[f]The nonequilibrium driving and track attachment break the Einstein relation between this D and ζ.

[g]Quantifying the precision highlights that a molecular machine could serve as a "clock",[180] and indeed, the distinction between a given system functioning as motor or as a clock may be fuzzy.[181]

REFERENCES

(1) Schrodinger, E. *What is Life?*; Cambridge University Press, 1944.
(2) Philips, R.; Kondev, J.; Theriot, J.; Garcia, H. *Physical Biology of the Cell*, 2nd ed.; Garland Science, 2012.
(3) Alberts, B.; Johnson, A.; Lewis, J.; Morgan, D.; Raff, M.; Roberts, K.; Walter, P. *Molecular Biology of the Cell*, 6th ed.; Garland Science, 2014.
(4) Kaldor, N. *The Theory of Capital*; Lutz: The Hague, The Netherlands, 1961; pp 177−222.
(5) Seifert, U. Stochastic thermodynamics, fluctuation theorems and molecular machines. *Rep. Prog. Phys.* **2012**, *75*, 126001.
(6) Jarzynski, C. Equalities and inequalities: Irreversibility and the second law of thermodynamics at the nanoscale. *Annu. Rev. Condens. Matter Phys.* **2011**, *2*, 329−351.
(7) Jülicher, F.; Ajdari, A.; Prost, J. Modeling molecular motors. *Rev. Mod. Phys.* **1997**, *69*, 1269−1281.
(8) Qian, H. The mathematical theory of molecular motor movement and chemomechanical energy transduction. *J. Math. Chem.* **2000**, *27*, 219−234.
(9) Bustamante, C.; Keller, D.; Oster, G. The physics of molecular motors. *Acc. Chem. Res.* **2001**, *34*, 412−420.
(10) Qian, H. Cycle kinetics, steady state thermodynamics and motors - a paradigm for living matter physics. *J. Phys.: Condens. Matter* **2005**, *17*, S3783−S3794.
(11) Kolomeisky, A. B.; Fisher, M. E. Molecular motors: A theorist's perspective. *Annu. Rev. Phys. Chem.* **2007**, *58*, 675−695.
(12) Astumian, R. D. Stochastic conformational pumping: A mechanism for free-energy transduction by molecules. *Annu. Rev. Biophys.* **2011**, *40*, 289−313.
(13) Kolomeisky, A. B. Motor proteins and molecular motors: how to operate machines at the nanoscale. *J. Phys.: Condens. Matter* **2013**, *25*, 463101.
(14) Chowdhury, D. Stochastic mechano-chemical kinetics of molecular motors: a multidisciplinary enterprise from a physicist's perspective. *Phys. Rep.* **2013**, *529*, 1−197.
(15) Chowdhury, D. Modeling stochastic kinetics of molecular machines at multiple levels: From molecules to modules. *Biophys. J.* **2013**, *104*, 2331−2341.
(16) Qian, H.; Kjelstrup, S.; Kolomeisky, A. B.; Bedeaux, D. Entropy production in mesoscopic stochastic thermodynamics: nonequilibrium kinetic cycles driven by chemical potentials, temperatures, and mechanical forces. *J. Phys.: Condens. Matter* **2016**, *28*, 153004.
(17) Hoffmann, P. M. How molecular motors extract order from chaos (a key issues review). *Rep. Prog. Phys.* **2016**, *79*, 032601.
(18) Goychuk, I. Molecular machines operating on the nanoscale: from classical to quantum. *Beilstein J. Nanotechnol.* **2016**, *7*, 328−350.
(19) Pezzato, C.; Cheng, C.; Stoddart, J. F.; Astumian, R. D. Mastering the non-equilibrium assembly and operation of molecular machines. *Chem. Soc. Rev.* **2017**, *46*, 5491−5507.
(20) Brown, A. I.; Sivak, D. A. Toward the design principles of molecular machines. *Physics in Canada* **2017**, *73*, 61−66.
(21) Astumian, R. D. Stochastically pumped adaptation and directional motion of molecular machines. *Proc. Natl. Acad. Sci. U. S. A.* **2018**, *115*, 9405−9413.
(22) Hirokawa, N.; Noda, Y.; Tanaka, Y.; Niwa, S. Kinesin superfamily motor proteins and intracellular transport. *Nat. Rev. Mol. Cell Biol.* **2009**, *10*, 682−696.
(23) Reck-Peterson, S. L.; Redwine, W. B.; Vale, R. D.; Carter, A. P. The cytoplasmic dynein transport machinery and its many cargoes. *Nat. Rev. Mol. Cell Biol.* **2018**, *19*, 382−398.
(24) Sellers, J. R. Myosins: a diverse superfamily. *Biochim. Biophys. Acta, Mol. Cell Res.* **2000**, *1496*, 3−22.
(25) Howard, J. *Mechanics of Motor Proteins and the Cytoskeleton*; Sinauer: Sunderland, MA, 2001.
(26) Rao, V. B.; Feiss, M. The bacteriophage DNA packaging motor. *Annu. Rev. Genet.* **2008**, *42*, 647−681.
(27) Singleton, M. R.; Dillingham, M. S.; Wigley, D. B. Structure and Mechanism of Helicases and Nucleic Acid Translocases. *Annu. Rev. Biochem.* **2007**, *76*, 23−50.
(28) Jorgensen, P. L.; Hakansson, K. O.; Karlish, S. J. D. Structure and mechanism of Na,K-ATPase: Functional sites and their interactions. *Annu. Rev. Physiol.* **2003**, *65*, 817−849.
(29) Berdis, A. J. Mechanisms of DNA Polymerases. *Chem. Rev.* **2009**, *109*, 2862−2879.
(30) Parker, J. In *Encyclopedia of Genetics*; Brenner, S., Miller, J. H., Eds.; Academic Press: New York, 2001; pp 1746−1747.
(31) Ramakrishnan, V. Ribosome structure and the mechanism of translation. *Cell* **2002**, *108*, 557−572.
(32) Junge, W.; Nelson, N. ATP synthase. *Annu. Rev. Biochem.* **2015**, *84*, 631−657.

DOI: 10.1021/acs.chemrev.9b00254
Chem. Rev. 2020, 120, 434−459

(33) Berg, H. C. Bacterial flagellar motor. *Curr. Biol.* **2008**, *18*, R689−R691.
(34) McLaughlin, R. T.; Diehl, M. R.; Kolomeisky, A. B. Collective dynamics of processive cytoskeletal motors. *Soft Matter* **2016**, *12*, 14−21.
(35) Hancock, W. O. Bidirectional cargo transport: moving beyond tug of war. *Nat. Rev. Mol. Cell Biol.* **2014**, *15*, 615−628.
(36) Baker, T. A.; Bell, S. P. Polymerases and the replisome: machines within machines. *Cell* **1998**, *92*, 295−305.
(37) Slochower, D. R.; Gilson, M. K. Motor-like properties of nonmotor enzymes. *Biophys. J.* **2018**, *114*, 2174−2179.
(38) Bustamante, C.; Chemla, Y. R.; Forde, N. R.; Izhaky, D. Mechanical processes in biochemistry. *Annu. Rev. Biochem.* **2004**, *73*, 705−748.
(39) Rondelez, Y.; Tresset, G.; Nakashima, T.; Kato-Yamada, Y.; Fujita, H.; Takeuchi, S.; Noji, H. Highly coupled ATP synthesis by F_1-ATPase single molecules. *Nature* **2005**, *433*, 773−777.
(40) Toyabe, S.; Watanabe-Nakayama, T.; Okamoto, T.; Kudo, S.; Muneyuki, E. Thermodynamic efficiency and mechanochemical coupling of F_1-ATPase. *Proc. Natl. Acad. Sci. U. S. A.* **2011**, *108*, 17951−17956.
(41) Yasuda, R.; Noji, H.; Kinosita, K.; Yoshida, M. F_1-ATPase is a highly efficient molecular motor that rotates with discrete 120° steps. *Cell* **1998**, *93*, 1117−1124.
(42) Kinosita, K., Jr; Yasuda, R.; Noji, H.; Adachi, K. A rotary molecular motor that can work at near 100% efficiency. *Philos. Trans. R. Soc., B* **2000**, *355*, 473−489.
(43) Boyer, P. D. The ATP synthase - A splendid molecular machine. *Annu. Rev. Biochem.* **1997**, *66*, 717−749.
(44) Kull, F. J.; Sablin, E. P.; Lau, R.; Fletterick, R. J.; Vale, R. D. Crystal structure of the kinesin motor domain reveals a structural similarity to myosin. *Nature* **1996**, *380*, 550−555.
(45) Jeney, S.; Stelzer, E. H. K.; Grubmüller, H.; Florin, E.-L. Mechanical properties of single motor molecules studied by three-dimensional thermal force probing in optical tweezers. *ChemPhysChem* **2004**, *5*, 1150−1158.
(46) Berman, H. M.; Westbrook, J.; Feng, Z.; Gilliland, G.; Bhat, T. N.; Weissig, H.; Shindyalov, I. N.; Bourne, P. E. The protein data bank. *Nucleic Acids Res.* **2000**, *28*, 235−242.
(47) Rastogi, V. K.; Girvin, M. E. Structural changes linked to proton translocation by subunit c of the ATP synthase. *Nature* **1999**, *402*, 263−268.
(48) Gibbons, C.; Montgomery, M. G.; Leslie, A. G. W.; Walker, J. E. The structure of the central stalk in bovine F_1-ATPase at 2.4 *Å* Resolution. *Nat. Struct. Biol.* **2000**, *7*, 1055−1061.
(49) Wilkens, S.; Borchardt, D.; Weber, J.; Senior, A. E. Structural characterization of the interaction of the δ and α subunits of the *Escherichia coli* F_1F_O-ATP Synthase by NMR Spectroscopy. *Biochemistry* **2005**, *44*, 11786−11794.
(50) Del Rizzo, P. A.; Bi, Y.; Dunn, S. D.; Shilton, B. H. The "second stalk" of *Escherichia coli* ATP synthase: structure of the isolated dimerization domain. *Biochemistry* **2002**, *41*, 6875−6884.
(51) Kozielski, F.; Sack, S.; Marx, A.; Thormahlen, M.; Schonbrunn, E.; Biou, V.; Thompson, A.; Mandelkow, E.-M.; Mandelkow, E. The crystal structure of dimeric kinesin and implications for microtubule-dependent motility. *Cell* **1997**, *91*, 985−994.
(52) Schnitzer, M. J.; Block, S. M. Kinesin hydrolyses one ATP per 8-nm step. *Nature* **1997**, *388*, 386−390.
(53) Coy, D. L.; Wagenbach, M.; Howard, J. Kinesin takes one 8-nm step for each ATP that it hydrolyzes. *J. Biol. Chem.* **1999**, *274*, 3667−3671.
(54) Svoboda, K.; Schmidt, C. F.; Schnapp, B. J.; Block, S. M. Direct observation of kinesin stepping by optical trapping interferometry. *Nature* **1993**, *365*, 721−727.
(55) Yildiz, A.; Tomishige, M.; Vale, R. D.; Selvin, P. R. Kinesin walks hand-over-hand. *Science* **2004**, *303*, 676−678.
(56) Andreasson, J. O. L.; Milic, B.; Chen, G.-Y.; Guydosh, N. R.; Hancock, W. O.; Block, S. M. Examining kinesin processivity within a general gating framework. *eLife* **2015**, *4*, No. e07403.
(57) Tomishige, M.; Stuurman, N.; Vale, R. D. Single-molecule observations of neck linker conformational changes in the kinesin motor protein. *Nat. Struct. Mol. Biol.* **2006**, *13*, 887−894.
(58) Zhang, Z.; Goldtzvik, Y.; Thirumalai, D. Parsing the roles of neck-linker docking and tethered head diffusion in the stepping dynamics of kinesin. *Proc. Natl. Acad. Sci. U. S. A.* **2017**, *114*, E9838−E9845.
(59) Cockburn, J. J. B.; Hesketh, S. J.; Mulhair, P.; Thomsen, M.; O'Connell, M. J.; Way, M. Insights into kinesin-1 activation from the crystal structure of KLC2 bound to JIP3. *Structure* **2018**, *26*, 1486−1498.
(60) Clancy, B. E.; Behnke-Parks, W. M.; Andreasson, J. O. L.; Rosenfeld, S. S.; Block, S. M. A universal pathway for kinesin stepping. *Nat. Struct. Mol. Biol.* **2011**, *18*, 1020−1027.
(61) Toprak, E.; Yildiz, A.; Hoffman, M. T.; Rosenfeld, S. S.; Selvin, P. R. Why kinesin is so processive. *Proc. Natl. Acad. Sci. U. S. A.* **2009**, *106*, 12717−12722.
(62) Baffou, G.; Rigneault, H.; Marguet, D.; Jullien, L. A critique of methods for temperature imaging in single cells. *Nat. Methods* **2014**, *11*, 899−901.
(63) Astumian, R. D. Design principles for Brownian molecular machines: how to swim in molasses and walk in a hurricane. *Phys. Chem. Chem. Phys.* **2007**, *9*, 5067−5083.
(64) Yanagida, T. Fluctuation as a tool of biological molecular machines. *BioSystems* **2008**, *93*, 3−7.
(65) Einstein, A. On the movement of small particles suspended in a stationary liquid demanded by the molecular kinetic theory of heat. *Ann. Phys.* **1905**, *322*, 549−560.
(66) Isojima, H.; Iino, R.; Niitani, Y.; Noji, H.; Tomishige, M. Direct observation of intermediate states during the stepping motion of kinesin-1. *Nat. Chem. Biol.* **2016**, *12*, 290−297.
(67) Chandler, D. *Introduction to Modern Statistical Mechanics*; Oxford University Press: Oxford, U.K., 1987.
(68) Harada, T.; Sasa, S.-I. Equality connecting energy dissipation with a violation of the fluctuation−response relation. *Phys. Rev. Lett.* **2005**, *95*, 130602.
(69) Seifert, U.; Speck, T. Fluctuation−dissipation theorem in nonequilibrium steady states. *Europhys. Lett.* **2010**, *89*, 10007.
(70) Verley, G.; Mallick, K.; Lacoste, D. Modified fluctuation−dissipation theorem for non-equilibrium steady states and applications to molecular motors. *Europhys. Lett.* **2011**, *93*, 10002.
(71) Purcell, E. M. Life at low Reynolds number. *Am. J. Phys.* **1977**, *45*, 3−11.
(72) Holzwarth, G.; Bonin, K.; Hill, D. B. Forces required of kinesin during processive transport through cytoplasm. *Biophys. J.* **2002**, *82*, 1784−1790.
(73) Ellis, R. J. Macromolecular crowding: obvious but underappreciated. *Trends Biochem. Sci.* **2001**, *26*, 597−604.
(74) Zhou, H. X.; Rivas, G.; Minton, A. P. Macromolecular crowding and confinement: biochemical, biophysical, and potential physiological consequences. *Annu. Rev. Biophys.* **2008**, *37*, 375−397.
(75) Hofling, F.; Franosch, T. Anomalous transport in the crowded world of biological cells. *Rep. Prog. Phys.* **2013**, *76*, 046602.
(76) Caragine, C. M.; Haley, S. C.; Zidovska, A. Surface fluctuations and coalescence of nucleolar droplets in the human cell nucleus. *Phys. Rev. Lett.* **2018**, *121*, 148101.
(77) Theillet, F.-X.; Binolfi, A.; Frembgen-Kesner, T.; Hingorani, K.; Sarkar, M.; Kyne, C.; Li, C.; Crowley, P. B.; Gierasch, L.; Pielak, G. J.; Elcock, A. H.; Gershenson, A.; Selenko, P. Physicochemical properties of cells and their effects on intrinsically disordered proteins (IDPs). *Chem. Rev.* **2014**, *114*, 6661−6714.
(78) Mahadevan, L.; Matsudaira, P. Motility powered by supramolecular springs and ratchets. *Science* **2000**, *288*, 95−100.
(79) Strasberg, P.; Schaller, G.; Lambert, N.; Brandes, T. Nonequilibrium thermodynamics in the strong coupling and non-Markovian regime based on a reaction coordinate mapping. *New J. Phys.* **2016**, *18*, 073007.
(80) Strasberg, P.; Esposito, M. Stochastic thermodynamics in the strong coupling regime: An unambiguous approach based on coarse

DOI: 10.1021/acs.chemrev.9b00254
Chem. Rev. 2020, 120, 434−459

graining. *Phys. Rev. E: Stat. Phys., Plasmas, Fluids, Relat. Interdiscip. Top.* **2017**, *95*, 062101.
(81) Seifert, U. First and second law of thermodynamics at strong coupling. *Phys. Rev. Lett.* **2016**, *116*, 020601.
(82) Jarzynski, C. Stochastic and macroscopic thermodynamics of strongly coupled systems. *Phys. Rev. X* **2017**, *7*, 011008.
(83) Junge, W.; Pänke, O.; Cherepanov, D. A.; Gumbiowski, K.; Muller, M.; Engelbrecht, S. Inter-subunit rotation and elastic power transmission in F_OF_1-ATPase. *FEBS Lett.* **2001**, *504*, 152−160.
(84) Sielaff, H.; Rennekamp, H.; Wächter, A.; Xie, H.; Hilbers, F.; Feldbauer, K.; Dunn, S. D.; Engelbrecht, S.; Junge, W. Domain compliance and elastic power transmission in rotary F_OF_1-ATPase. *Proc. Natl. Acad. Sci. U. S. A.* **2008**, *105*, 17760−17765.
(85) Junge, W.; Sielaff, H.; Engelbrecht, S. Torque generation and elastic power transmission in the rotary F_OF_1-ATPase. *Nature* **2009**, *459*, 364−370.
(86) Okuno, D.; Iino, R.; Noji, H. Stiffness of γ subunit of F_1-ATPase. *Eur. Biophys. J.* **2010**, *39*, 1589−1596.
(87) Wächter, A.; Bi, Y.; Dunn, S. D.; Cain, B. D.; Sielaff, H.; Wintermann, F.; Engelbrecht, S.; Junge, W. Two rotary motors in F-ATP synthase are elastically coupled by a flexible rotor and a stiff stator stalk. *Proc. Natl. Acad. Sci. U. S. A.* **2011**, *108*, 3924−3929.
(88) Czub, J.; Grubmüller, H. Torsional elasticity and energetics of F_1-ATPase. *Proc. Natl. Acad. Sci. U. S. A.* **2011**, *108*, 7408−7413.
(89) Okazaki, K.-I.; Hummer, G. Elasticity, friction, and pathway of γ-subunit rotation in F_OF_1-ATP synthase. *Proc. Natl. Acad. Sci. U. S. A.* **2015**, *112*, 10720−10725.
(90) Onsager, L. Reciprocal relations in irreversible processes. *Phys. Rev.* **1931**, *37*, 405−426.
(91) Astumian, R. D. Microscopic reversibility as the organizing principle of molecular machines. *Nat. Nanotechnol.* **2012**, *7*, 684−688.
(92) Diez, M.; Zimmermann, B.; Börsch, M.; König, M.; Schweinberger, E.; Steigmiller, S.; Reuter, R.; Felekyan, S.; Kudryavtsev, V.; Seidel, C. A. M.; Gräber, P. Proton-powered subunit rotation in single membrane-bound F_OF_1-ATP synthase. *Nat. Struct. Mol. Biol.* **2004**, *11*, 135−141.
(93) Hackney, D. D. The tethered motor domain of a kinesin-microtubule complex catalyzes reversible synthesis of bound ATP. *Proc. Natl. Acad. Sci. U. S. A.* **2005**, *102*, 18338−18343.
(94) Sellers, J. R.; Veigel, C. Direct observation of the myosin-Va power stroke and its reversal. *Nat. Struct. Mol. Biol.* **2010**, *17*, 590−595.
(95) Gebhardt, J. C. M.; Clemen, A. E.-M.; Jaud, J.; Rief, M. Myosin-V is a mechanical ratchet. *Proc. Natl. Acad. Sci. U. S. A.* **2006**, *103*, 8680−8685.
(96) Carter, N. J.; Cross, R. A. Mechanics of the kinesin step. *Nature* **2005**, *435*, 308−312.
(97) van Kampen, N. *Stochastic Processes in Physics and Chemistry*, 3rd ed.; North Holland, 2007.
(98) Feynman, R. P.; Leighton, R. B.; Sands, M. *The Feynman Lectures on Physics*; Addison-Wesley, 1966.
(99) Jarzynski, C.; Mazonka, O. Feynman's ratchet and pawl: an exactly solvable model. *Phys. Rev. E: Stat. Phys., Plasmas, Fluids, Relat. Interdiscip. Top.* **1999**, *59*, 6448−6459.
(100) Tu, Z. C. Efficiency at maximum power of Feynman's ratchet as a heat engine. *J. Phys. A: Math. Theor.* **2008**, *41*, 312003.
(101) Ariga, T.; Tomishige, M.; Mizuno, D. Nonequilibrium energetics of molecular motor kinesin. *Phys. Rev. Lett.* **2018**, *121*, 218101.
(102) Machta, B. B. Dissipation bound for thermodynamic control. *Phys. Rev. Lett.* **2015**, *115*, 260603.
(103) Milo, R.; Phillips, R. *Cell Biology by the Numbers*; Garland Science, 2015.
(104) Zhang, Y. The efficiency of molecular motors. *J. Stat. Phys.* **2009**, *134*, 669−679.
(105) Gardiner, C. *Handbook of Stochastic Methods*; Springer, 2004.
(106) Risken, H. *The Fokker−Planck Equation: Methods of Solution and Applications*, 3rd ed.; Springer, 1996.
(107) Frenkel, D.; Smit, B. *Understanding Molecular Simulation*, 2nd ed.; Academic Press, 2002.
(108) Sivak, D. A.; Chodera, J. D.; Crooks, G. E. Using nonequilibrium fluctuation theorems to understand and correct errors in equilibrium and nonequilibrium simulations of discrete Langevin dynamics. *Phys. Rev. X* **2013**, *3*, 011007.
(109) Sivak, D. A.; Chodera, J. D.; Crooks, G. E. Time step rescaling recovers continuous-time dynamical properties for discrete-time Langevin integration of nonequilibrium systems. *J. Phys. Chem. B* **2014**, *118*, 6466−6474.
(110) van Kampen, N. Elimination of fast variables. *Phys. Rep.* **1985**, *124*, 69−160.
(111) Mukherjee, S.; Alhadeff, R.; Warshel, A. Simulating the dynamics of the mechanochemical cycle of myosin-V. *Proc. Natl. Acad. Sci. U. S. A.* **2017**, *114*, 2259−2264.
(112) Doering, C. R. Randomly rattled ratchets. *Nuovo Cimento Soc. Ital. Fis., D* **1995**, *17*, 685−697.
(113) Kedem, O.; Lau, B.; Ratner, M. A.; Weiss, E. A. Light-responsive organic flashing electron ratchet. *Proc. Natl. Acad. Sci. U. S. A.* **2017**, *114*, 8698−8703.
(114) Mel'nikov, V. I. The Kramers problem: Fifty years of development. *Phys. Rep.* **1991**, *209*, 1−71.
(115) Qian, H. A simple theory of motor protein kinetics and energetics. *Biophys. Chem.* **1997**, *67*, 263−267.
(116) Challis, K. J. Tight-binding derivation of a discrete-continuous description of mechanochemical coupling in a molecular motor. *Phys. Rev. E: Stat. Phys., Plasmas, Fluids, Relat. Interdiscip. Top.* **2018**, *97*, 062158.
(117) Xing, J.; Liao, J.-C.; Oster, G. Making ATP. *Proc. Natl. Acad. Sci. U. S. A.* **2005**, *102*, 16539−16546.
(118) Xing, J.; Wang, H.; Oster, G. From continuum Fokker−Planck models to discrete kinetic models. *Biophys. J.* **2005**, *89*, 1551−1563.
(119) Ovchinnikov, V.; Karplus, M.; Vanden-Eijnden, E. Free energy of conformational transition paths in biomolecules: The string method and its application to myosin VI. *J. Chem. Phys.* **2011**, *134*, 085103.
(120) Czub, J.; Wieczór, M.; Prokopowicz, B.; Grubmüller, H. Mechanochemical energy transduction during the main rotary step in the synthesis cycle of F_1-ATPase. *J. Am. Chem. Soc.* **2017**, *139*, 4025−4034.
(121) Dai, L.; Flechsig, H.; Yu, J. Deciphering intrinsic inter-subunit couplings that lead to sequential hydrolysis of F_1-ATPase ring. *Biophys. J.* **2017**, *113*, 1440−1453.
(122) Pu, J.; Karplus, M. How subunit coupling produces the γ-subunit rotary motion in F_1-ATPase. *Proc. Natl. Acad. Sci. U. S. A.* **2008**, *105*, 1192−1197.
(123) Mukherjee, S.; Bora, R. P.; Warshel, A. Torque, chemistry and efficiency in molecular motors: a study of the rotary-chemical coupling in F_1-ATPase. *Q. Rev. Biophys.* **2015**, *48*, 395−403.
(124) Isaka, Y.; Ekimoto, T.; Kokabu, Y.; Yamato, I.; Murata, T.; Ikeguchi, M. Rotation Mechanism of Molecular Motor V1-ATPase Studied by Multiscale Molecular Dynamics Simulation. *Biophys. J.* **2017**, *112*, 911−920.
(125) Trepagnier, E. H.; Jarzynski, C.; Ritort, F.; Crooks, G. E.; Bustamante, C. J.; Liphardt, J. Experimental test of Hatano and Sasa's nonequilibrium steady-state equality. *Proc. Natl. Acad. Sci. U. S. A.* **2004**, *101*, 15038−15041.
(126) Hill, T. *Free Energy Transduction in Biology: Steady State Kinetic and Thermodynamic Formalism*; Academic Press, 1977.
(127) Koza, Z. General technique of calculating the drift velocity and diffusion coefficient in arbitrary periodic systems. *J. Phys. A: Math. Gen.* **1999**, *32*, 7637−7651.
(128) Koza, Z. Diffusion coefficient and drift velocity in periodic media. *Phys. A* **2000**, *285*, 176−186.
(129) Chemla, Y. R.; Moffitt, J. R.; Bustamante, C. Exact solutions for kinetic models of macromolecular dynamics. *J. Phys. Chem. B* **2008**, *112*, 6025−6044.

DOI: 10.1021/acs.chemrev.9b00254
Chem. Rev. 2020, 120, 434−459

(130) Sivaramakrishnan, S.; Sung, J. M.; Dunn, A. R.; Spudich, J. A. Dual-Beam Optical Tweezers. In *Encyclopedia of Biophysics*; Roberts, G. C. K., Ed.; Springer: Berlin, 2013; pp 522−526.
(131) Barato, A. C.; Seifert, U. Thermodynamic uncertainty relation for biomolecular processes. *Phys. Rev. Lett.* **2015**, *114*, 158101.
(132) Crooks, G. E. Entropy production fluctuation theorem and the nonequilibrium work relation for free energy differences. *Phys. Rev. E: Stat. Phys., Plasmas, Fluids, Relat. Interdiscip. Top.* **1999**, *60*, 2721−2726.
(133) Lacoste, D.; Mallick, K. Fluctuation Relations for Molecular Motors. *Prog. Math. Phys.* **2011**, *60*, 61−88.
(134) Schmiedl, T.; Seifert, U. Efficiency of molecular motors at maximum power. *Europhys. Lett.* **2008**, *83*, 30005.
(135) Elms, P. J.; Chodera, J. D.; Bustamante, C.; Marqusee, S. The molten globule state is unusually deformable under mechanical force. *Proc. Natl. Acad. Sci. U. S. A.* **2012**, *109*, 3796−3801.
(136) Wagoner, J. A.; Dill, K. A. Molecular motors: Power strokes outperform Brownian ratchets. *J. Phys. Chem. B* **2016**, *120*, 6327−6336.
(137) Brown, A. I.; Sivak, D. A. Allocating and splitting free energy to maximize molecular machine flux. *J. Phys. Chem. B* **2018**, *122*, 1387−1393.
(138) Astumian, R. D. Optical vs. chemical driving for molecular machines. *Faraday Discuss.* **2016**, *195*, 583−597.
(139) Howard, J. Motor Proteins as Nanomachines: The Roles of Thermal Fluctuations in Generating Force and Motion. *Prog. Math. Phys.* **2011**, *60*, 47−59.
(140) Amos, L. A. Molecular motors: not quite like clockwork. *Cell. Mol. Life Sci.* **2008**, *65*, 509−515.
(141) Qian, H. Vector field formalism and analysis for a class of thermal ratchets. *Phys. Rev. Lett.* **1998**, *81*, 3063−3066.
(142) Geeves, M. A.; Fedorov, R.; Manstein, D. J. Molecular mechanism of actomyosin-based motility. *Cell. Mol. Life Sci.* **2005**, *62*, 1462−1477.
(143) Miyashita, O.; Onuchic, J. N.; Wolynes, P. G. Nonlinear elasticity, proteinquakes, and the energy landscapes of functional transitions in proteins. *Proc. Natl. Acad. Sci. U. S. A.* **2003**, *100*, 12570−12575.
(144) Koga, N.; Takada, S. Folding-based molecular simulations reveal mechanisms of the rotary motor F_1ATPase. *Proc. Natl. Acad. Sci. U. S. A.* **2006**, *103*, 5367−5372.
(145) Mickler, M.; Hessling, M.; Ratzke, C.; Buchner, J.; Hugel, T. The large conformational changes of Hsp90 are only weakly coupled to ATP hydrolysis. *Nat. Struct. Mol. Biol.* **2009**, *16*, 281−286.
(146) Kondo, H. X.; Okimoto, N.; Morimoto, G.; Taiji, M. Free-energy landscapes of protein domain movements upon ligand binding. *J. Phys. Chem. B* **2011**, *115*, 7629−7636.
(147) Zwanzig, R. *Nonequilibrium Statistical Mechanics*; Oxford University Press: New York, 2001.
(148) Sivak, D. A.; Crooks, G. E. Thermodynamic metrics and optimal paths. *Phys. Rev. Lett.* **2012**, *108*, 190602.
(149) Schroeder, D. *An Introduction to Thermal Physics*; Addison Wesley, 1999.
(150) Parmeggiani, A.; Jülicher, F.; Ajdari, A.; Prost, J. Energy transduction of isothermal ratchets: generic aspects and specific examples close to and far from equilibrium. *Phys. Rev. E: Stat. Phys., Plasmas, Fluids, Relat. Interdiscip. Top.* **1999**, *60*, 2127−2140.
(151) Seifert, U. Efficiency of autonomous soft nanomachines at maximum power. *Phys. Rev. Lett.* **2011**, *106*, 020601.
(152) Oster, G.; Wang, H. H. Reverse engineering a protein: The mechanochemistry of ATP synthase. *Biochim. Biophys. Acta, Bioenerg.* **2000**, *1458*, 482−510.
(153) Wang, H.; Oster, G. The Stokes efficiency for molecular motors and its applications. *Europhys. Lett.* **2002**, *57*, 134.
(154) Van den Broeck, C.; Kumar, N.; Lindenberg, K. Efficiency of isothermal molecular machines at maximum power. *Phys. Rev. Lett.* **2012**, *108*, 210602.
(155) Verley, G.; Willaert, T.; Van den Broeck, C.; Esposito, M. Universal theory of efficiency fluctuations. *Phys. Rev. E* **2014**, *90*, 052145.
(156) Manikandan, S. K.; Dabelow, L.; Eichhorn, R.; Krishnamurthy, S. Efficiency fluctuations in microscopic machines. *Phys. Rev. Lett.* **2019**, *122*, 140601.
(157) Derenyi, I.; Bier, M.; Astumian, R. D. Generalized efficiency and its application to microscopic engines. *Phys. Rev. Lett.* **1999**, *83*, 903−906.
(158) Lau, A. W. C.; Lacoste, D.; Mallick, K. Nonequilibrium fluctuations and mechanochemical couplings of a molecular motor. *Phys. Rev. Lett.* **2007**, *99*, 158102.
(159) Pietzonka, P.; Barato, A. C.; Seifert, U. Universal bound on the efficiency of molecular motors. *J. Stat. Mech.: Theory Exp.* **2016**, *2016*, 124004.
(160) Golubeva, N.; Imparato, A. Efficiency at maximum power of interacting molecular machines. *Phys. Rev. Lett.* **2012**, *109*, 190602.
(161) Golubeva, N.; Imparato, A. Maximum power operation of interacting molecular motors. *Phys. Rev. E* **2013**, *88*, 012114.
(162) Silverstein, T. P. An exploration of how the thermodynamic efficiency of bioenergetic membrane systems varies with c-subunit stoichiometry of F_1F_O ATP synthases. *J. Bioenerg. Biomembr.* **2014**, *46*, 229−241.
(163) Hua, W.; Young, E. C.; Fleming, M. L.; Gelles, J. Coupling of kinesin steps to ATP hydrolysis. *Nature* **1997**, *388*, 390−393.
(164) Fisher, M. E.; Kolomeisky, A. B. The force exerted by a molecular motor. *Proc. Natl. Acad. Sci. U. S. A.* **1999**, *96*, 6597−6602.
(165) Darnton, N. C.; Turner, L.; Rojevsky, S.; Berg, H. C. On torque and tumbling in swimming Escherichia coli. *J. Bacteriol.* **2007**, *189*, 1756−1764.
(166) Berg, H. C.; Turner, L. Torque generated by the flagellar motor of Escherichia coli. *Biophys. J.* **1993**, *65*, 2201−2216.
(167) Ueno, H.; Suzuki, T.; Kinosita, K.; Yoshida, M. ATP-driven stepwise rotation of F_OF_1-ATP synthase. *Proc. Natl. Acad. Sci. U. S. A.* **2005**, *102*, 1333−1338.
(168) Tominaga, M.; Kojima, H.; Yokota, E.; Orii, H.; Nakamori, R.; Katayama, E.; Anson, M.; Shimmen, T.; Oiwa, K. Higher plant myosin XI moves processively on actin with 35 nm steps at high velocity. *EMBO J.* **2003**, *22*, 1263−1272.
(169) Banerjee, K.; Kolomeisky, A. B.; Igoshin, O. A. Elucidating interplay of speed and accuracy in biological error correction. *Proc. Natl. Acad. Sci. U. S. A.* **2017**, *114*, 5183−5188.
(170) Nguyen, V.; Wilson, C.; Hoemberger, M.; Stiller, J. B.; Agafonov, R. V.; Kutter, S.; English, J.; Theobald, D. L.; Kern, D. Evolutionary drivers of thermoadaptation in enzyme catalysis. *Science* **2017**, *355*, 289−294.
(171) Albery, W. J.; Knowles, J. R. Evolution of enzyme function and the development of catalytic efficiency. *Biochemistry* **1976**, *15*, 5631−5640.
(172) Lan, G.; Sartori, P.; Neumann, S.; Sourjik, V.; Tu, Y. The energy-speed-accuracy trade-off in sensory adaptation. *Nat. Phys.* **2012**, *8*, 422−428.
(173) Fisher, M. E.; Kolomeisky, A. B. Simple mechanochemistry describes the dynamics of kinesin molecules. *Proc. Natl. Acad. Sci. U. S. A.* **2001**, *98*, 7748−7753.
(174) Lipowsky, R.; Klumpp, S. 'Life is motion': Multiscale motility of molecular motors. *Phys. A* **2005**, *352*, 53−112.
(175) Brown, A. I.; Sivak, D. A. Allocating dissipation across a molecular machine cycle to maximize flux. *Proc. Natl. Acad. Sci. U. S. A.* **2017**, *114*, 11057−11062.
(176) Hwang, W.; Hyeon, C. Quantifying the heat dissipation from a molecular motor's transport properties in nonequilibrium steady states. *J. Phys. Chem. Lett.* **2017**, *8*, 250−256.
(177) Anandakrishnan, R.; Zhang, Z.; Donovan-Maiye, R.; Zuckerman, D. M. Biophysical comparison of ATP synthesis mechanisms shows a kinetic advantage for the rotary process. *Proc. Natl. Acad. Sci. U. S. A.* **2016**, *113*, 11220−11225.

DOI: 10.1021/acs.chemrev.9b00254
Chem. Rev. 2020, 120, 434−459

(178) Wagoner, J. A.; Dill, K. A. Mechanisms for achieving high speed and efficiency in biomolecular machines. *Proc. Natl. Acad. Sci. U. S. A.* **2019**, *116*, 5902−5907.
(179) Fano, U. Ionization Yield of Radiations. II. The Fluctuations of the Number of Ions. *Phys. Rev.* **1947**, *72*, 26−29.
(180) Barato, A. C.; Seifert, U. Cost and precision of Brownian clocks. *Phys. Rev. X* **2016**, *6*, 041053.
(181) Hess, H. Molecular Motor or Molecular Clock: A Question of Load. 2017, arXiv:1709.09054 [physics.chem-ph]. arXiv.org e-Print archive. https://arxiv.org/abs/1709.09054.
(182) Svoboda, K.; Mitra, P. P.; Block, S. M. Fluctuation analysis of motor protein movement and single enzyme kinetics. *Proc. Natl. Acad. Sci. U. S. A.* **1994**, *91*, 11782−11786.
(183) Visscher, K.; Schnitzer, M. J.; Block, S. M. Single kinesin molecules studied with a molecular force clamp. *Nature* **1999**, *400*, 184−189.
(184) Block, S. M.; Asbury, C. L.; Shaevitz, J. W.; Lang, M. J. Probing the kinesin reaction cycle with a 2D optical force clamp. *Proc. Natl. Acad. Sci. U. S. A.* **2003**, *100*, 2351−2356.
(185) Koza, Z. General relation between drift velocity and dispersion of a molecular motor. *Acta Phys. Pol., B* **2002**, *33*, 1025−1030.
(186) Koza, Z. Maximal force exerted by a molecular motor. *Phys. Rev. E: Stat. Phys., Plasmas, Fluids, Relat. Interdiscip. Top.* **2002**, *65*, 031905.
(187) Barato, A. C.; Seifert, U. Universal bound on the Fano factor in enzyme kinetics. *J. Phys. Chem. B* **2015**, *119*, 6555−6561.
(188) Gingrich, T. R.; Horowitz, J. M.; Perunov, N.; England, J. L. Dissipation bounds all steady-state current fluctuations. *Phys. Rev. Lett.* **2016**, *116*, 120601.
(189) Pietzonka, P.; Ritort, F.; Seifert, U. Finite-time generalization of the thermodynamic uncertainty relation. *Phys. Rev. E: Stat. Phys., Plasmas, Fluids, Relat. Interdiscip. Top.* **2017**, *96*, 012101.
(190) Horowitz, J. M.; Gingrich, T. R. Proof of the finite-time thermodynamic uncertainty relation for steady-state currents. *Phys. Rev. E: Stat. Phys., Plasmas, Fluids, Relat. Interdiscip. Top.* **2017**, *96*, 020103.
(191) Proesmans, K.; Van den Broeck, C. Discrete-time thermodynamic uncertainty relation. *EPL* **2017**, *119*, 20001.
(192) Polettini, M.; Lazarescu, A.; Esposito, M. Tightening the uncertainty principle for stochastic currents. *Phys. Rev. E: Stat. Phys., Plasmas, Fluids, Relat. Interdiscip. Top.* **2016**, *94*, 052104.
(193) Zimmermann, E.; Seifert, U. Efficiencies of a molecular motor: a generic hybrid model applied to the F_1-ATPase. *New J. Phys.* **2012**, *14*, 103023.
(194) Zimmermann, E.; Seifert, U. Effective rates from thermodynamically consistent coarse-graining of models for molecular motors with probe particles. *Phys. Rev. E* **2015**, *91*, 022709.
(195) Zimmermann, E. Dynamics and Thermodynamics of Molecular Motor−Cargo Systems. Doctoral Thesis, Universität Stuttgart, Stuttgart, Germany, 2015.
(196) Brown, A. I.; Sivak, D. A. Pulling cargo increases the precision of molecular motor progress. *Europhys. Lett.* **2019**, *126*, 40004.
(197) Pietzonka, P.; Seifert, U. Universal trade-off between power, efficiency, and constancy in steady-state heat engines. *Phys. Rev. Lett.* **2018**, *120*, 190602.
(198) Ouldridge, T. E.; Govern, C. C.; ten Wolde, P. R. Thermodynamics of computational copying in biochemical systems. *Phys. Rev. X* **2017**, *7*, 021004.
(199) Nguyen, M.; Vaikuntanathan, S. Design principles for nonequilibrium self-assembly. *Proc. Natl. Acad. Sci. U. S. A.* **2016**, *113*, 14231−14236.
(200) Hwang, W.; Hyeon, C. Energetic costs, precision, and transport efficiency of molecular motors. *J. Phys. Chem. Lett.* **2018**, *9*, 513−520.
(201) Hyeon, C.; Hwang, W. Physical insight into the thermodynamic uncertainty relation using Brownian motion in tilted periodic potentials. *Phys. Rev. E: Stat. Phys., Plasmas, Fluids, Relat. Interdiscip. Top.* **2017**, *96*, 012156.
(202) Qian, H. Motor protein with nonequilibrium potential: Its thermodynamics and efficiency. *Phys. Rev. E* **2004**, *69*, 012901.
(203) Qian, H. A simple theory of motor protein kinetics and energetics. II. *Biophys. Chem.* **2000**, *83*, 35−43.
(204) Cappello, G.; Pierobon, P.; Symonds, C.; Busoni, L.; Christof, J.; Gebhardt, M.; Rief, M.; Prost, J. Myosin V stepping mechanism. *Proc. Natl. Acad. Sci. U. S. A.* **2007**, *104*, 15328−15333.
(205) Nicholas, M. P.; Höök, P.; Brenner, S.; Wynne, C. L.; Vallee, R. B.; Gennerich, A. Control of cytoplasmic dynein force production and processivity by its C-terminal domain. *Nat. Commun.* **2015**, *6*, 6206.
(206) Wang, M. D.; Schnitzer, M. J.; Yin, H.; Landick, R.; Gelles, J.; Block, S. M. Force and velocity measured for single molecules of RNA polymerase. *Science* **1998**, *282*, 902−907.
(207) Sakamoto, T.; Wang, F.; Schmitz, S.; Xu, Y.; Xu, Q.; Molloy, J. E.; Veigel, C.; Sellers, J. R. Neck length and processivity of myosin V. *J. Biol. Chem.* **2003**, *278*, 29201−29207.
(208) Alon, U. *An Introduction to Systems Biology: Design Principles of Biological Circuits*; CRC Press: Boca Raton, FL, 2006.
(209) Shoval, O.; Sheftel, H.; Shinar, G.; Hart, Y.; Ramote, O.; Mayo, A.; Dekel, E.; Kavanagh, K.; Alon, U. Evolutionary trade-offs, Pareto optimality, and the geometry of phenotype space. *Science* **2012**, *336*, 1157−1160.
(210) Sheftel, H.; Shoval, O.; Mayo, A.; Alon, U. The geometry of the Pareto front in biological phenotype space. *Ecol. Evol.* **2013**, *3*, 1471−1483.
(211) Solon, A. P.; Horowitz, J. M. Phase transition in protocols minimizing work fluctuations. *Phys. Rev. Lett.* **2018**, *120*, 180605.
(212) Hopfield, J. Kinetic proofreading − new mechanism for reducing errors in biosynthetic processes requiring high specificity. *Proc. Natl. Acad. Sci. U. S. A.* **1974**, *71*, 4135−4139.
(213) Ninio, J. Kinetic amplification of enzyme discrimination. *Biochimie* **1975**, *57*, 587−595.
(214) Murugan, A.; Huse, D. A.; Leibler, S. Speed, dissipation, and error in kinetic proofreading. *Proc. Natl. Acad. Sci. U. S. A.* **2012**, *109*, 12034−12039.
(215) McKeithan, T. W. Kinetic proofreading in T-cell receptor signal transduction. *Proc. Natl. Acad. Sci. U. S. A.* **1995**, *92*, 5042−5046.
(216) Francois, P.; Voisinne, G.; Siggia, E. D.; Altan-Bonnet, G.; Vergassola, M. Phenotypic model for early T-cell activation displaying sensitivity, specificity, and antagonism. *Proc. Natl. Acad. Sci. U. S. A.* **2013**, *110*, E888−E897.
(217) Sartori, P.; Tu, Y. Free energy cost of reducing noise while maintaining a high sensitivity. *Phys. Rev. Lett.* **2015**, *115*, 118102.
(218) Mehta, P.; Schwab, D. J. Energetic costs of cellular computation. *Proc. Natl. Acad. Sci. U. S. A.* **2012**, *109*, 17978−17982.
(219) Feng, E. H.; Crooks, G. E. Length of time's arrow. *Phys. Rev. Lett.* **2008**, *101*, 090602.
(220) Cover, T. M.; Thomas, J. A. *Elements of Information Theory*, 2nd ed.; Wiley-Interscience: Hoboken, NJ, 2006.
(221) Lacasa, L.; Nunez, A.; Roldan, E.; Parrondo, J. M. R.; Luque, B. Time series irreversibility: A visibility graph approach. *Eur. Phys. J. B* **2012**, *85*, 217.
(222) Roldan, E.; Parrondo, J. M. R. Entropy production and Kullback-Leibler divergence between stationary trajectories of discrete systems. *Phys. Rev. E* **2012**, *85*, 031129.
(223) Crooks, G. E.; Sivak, D. A. Measures of trajectory ensemble disparity in nonequilibrium statistical dynamics. *J. Stat. Mech.: Theory Exp.* **2011**, *2011*, P06003.
(224) Collin, D.; Ritort, F.; Jarzynski, C.; Smith, S. B.; Tinoco, J. I.; Bustamante, C. Verification of the Crooks fluctuation theorem and recovery of RNA folding free energies. *Nature* **2005**, *437*, 231−234.
(225) Procacci, P.; Marsili, S. Energy dissipation asymmetry in the non equilibrium folding/unfolding of the single molecule alanine decapeptide. *Chem. Phys.* **2010**, *375*, 8−15.
(226) Brown, A. I.; Sivak, D. A. Effective dissipation: Breaking time-reversal symmetry in driven microscopic energy transmission. *Phys.*

DOI: 10.1021/acs.chemrev.9b00254
Chem. Rev. 2020, 120, 434−459

Rev. E: Stat. Phys., Plasmas, Fluids, Relat. Interdiscip. Top. **2016**, *94*, 032137.
(227) Zarrin, A.; Sivak, D. A.; Brown, A. I. Breaking time-reversal symmetry for ratchet models of molecular machines. *Phys. Rev. E: Stat. Phys., Plasmas, Fluids, Relat. Interdiscip. Top.* **2019**, *99*, 062127.
(228) Roldan, É.; Neri, I.; Dorpinghaus, M.; Meyr, H.; Jülicher, F. Decision making in the arrow of time. *Phys. Rev. Lett.* **2015**, *115*, 250602.
(229) Tafoya, S.; Large, S. J.; Liu, S.; Bustamante, C.; Sivak, D. A. Using a system's equilibrium behavior to reduce its energy dissipation in nonequilibrium processes. *Proc. Natl. Acad. Sci. U. S. A.* **2019**, *116*, 5920−5924.
(230) Kubo, R. Statistical-mechanical theory of irreversible processes. 1. General theory and simple applications to magnetic and conduction problems. *J. Phys. Soc. Jpn.* **1957**, *12*, 570−586.
(231) Schmiedl, T.; Seifert, U. Optimal finite-time processes in stochastic thermodynamics. *Phys. Rev. Lett.* **2007**, *98*, 108301.
(232) Gomez-Marin, A.; Schmiedl, T.; Seifert, U. Optimal protocols for minimal work processes in underdamped stochastic thermodynamics. *J. Chem. Phys.* **2008**, *129*, 024114.
(233) Aurell, E.; Mejia-Monasterio, C.; Muratore-Ginanneschi, P. Optimal protocols and optimal transport in stochastic thermodynamics. *Phys. Rev. Lett.* **2011**, *106*, 250601.
(234) Zulkowski, P. R.; Sivak, D. A.; Crooks, G. E.; DeWeese, M. R. Geometry of thermodynamic control. *Phys. Rev. E* **2012**, *86*, 041148.
(235) Zulkowski, P. R.; DeWeese, M. R. Optimal finite-time erasure of a classical bit. *Phys. Rev. E* **2014**, *89*, 052140.
(236) Bonança, M. V. S.; Deffner, S. Optimal driving of isothermal processes close to equilibrium. *J. Chem. Phys.* **2014**, *140*, 244119.
(237) Rotskoff, G. M.; Crooks, G. E. Optimal control in nonequilibrium systems: Dynamic Riemannian geometry of the Ising model. *Phys. Rev. E* **2015**, *92*, 060102.
(238) Zulkowski, P. R.; DeWeese, M. R. Optimal control of overdamped systems. *Phys. Rev. E* **2015**, *92*, 032117.
(239) Rotskoff, G. M.; Crooks, G. E.; Vanden-Eijnden, E. Geometric approach to optimal nonequilibrium control: Minimizing dissipation in nanomagnetic spin systems. *Phys. Rev. E: Stat. Phys., Plasmas, Fluids, Relat. Interdiscip. Top.* **2017**, *95*, 012148.
(240) Bonança, M. V. S.; Deffner, S. Minimal dissipation in processes far from equilibrium. *Phys. Rev. E: Stat. Phys., Plasmas, Fluids, Relat. Interdiscip. Top.* **2018**, *98*, 042103.
(241) Sivak, D. A.; Crooks, G. E. Thermodynamic geometry of minimum-dissipation driven barrier crossing. *Phys. Rev. E: Stat. Phys., Plasmas, Fluids, Relat. Interdiscip. Top.* **2016**, *94*, 052106.
(242) Mandal, D.; Jarzynski, C. Analysis of slow transitions between nonequilibrium steady states. *J. Stat. Mech.: Theory Exp.* **2016**, *2016*, 063204.
(243) Zulkowski, P. R.; Sivak, D. A.; DeWeese, M. R. Optimal control of transitions between nonequilibrium steady states. *PLoS One* **2013**, *8*, No. e82754.
(244) Lucero, J. N. E.; Mehdizadeh, A.; Sivak, D. A. Optimal control of rotary motors. *Phys. Rev. E: Stat. Phys., Plasmas, Fluids, Relat. Interdiscip. Top.* **2019**, *99*, 012119.
(245) Blaber, S.; Sivak, D. A. Optimal control of protein copy number. 2018, arXiv:1810.02046 [q-bio.SC]. arXiv.org e-Print archive. https://arxiv.org/abs/1810.02046.
(246) Liu, S.; Chistol, G.; Hetherington, C. L.; Tafoya, S.; Aathavan, K.; Schnitzbauer, J.; Grimes, S.; Jardine, P. J.; Bustamante, C. A viral packaging motor varies its DNA rotation and step size to preserve subunit coordination as the capsid fills. *Cell* **2014**, *157*, 702−713.
(247) Berndsen, Z. T.; Keller, N.; Grimes, S.; Jardine, P. J.; Smith, D. E. Nonequilibrium dynamics and ultraslow relaxation of confined DNA during viral packaging. *Proc. Natl. Acad. Sci. U. S. A.* **2014**, *111*, 8345−8350.
(248) Chen, J.; Coakley, A.; O'Connor, M.; Petrov, A.; O'Leary, S. E.; Atkins, J. F.; Puglisi, J. D. Coupling of mRNA structure rearrangement to ribosome movement during bypassing of non-coding regions. *Cell* **2015**, *163*, 1267−1280.
(249) Large, S. J.; Chetrite, R.; Sivak, D. A. Stochastic control in microscopic nonequilibrium systems. *Europhys. Lett.* **2018**, *124*, 20001.
(250) Large, S. J.; Sivak, D. A. Optimal discrete control: minimizing dissipation in discretely driven nonequilibrium systems. *J. Stat. Mech.: Theory Exp.* 2019, in press; arXiv:1812.08216 [cond-mat.stat-mech]. arXiv.org e-Print archive. https://arxiv.org/abs/1812.08216.
(251) Rao, R.; Esposito, M. Nonequilibrium thermodynamics of chemical reaction networks: Wisdom from stochastic thermodynamics. *Phys. Rev. X* **2016**, *6*, 041064.
(252) Rao, R.; Esposito, M. Conservation laws shape dissipation. *New J. Phys.* **2018**, *20*, 023007.
(253) Rao, R.; Esposito, M. Conservation laws and work fluctuation relations in chemical reaction networks. *J. Chem. Phys.* **2018**, *149*, 245101−26.
(254) Verley, G.; Van den Broeck, C.; Esposito, M. Work statistics in stochastically driven systems. *New J. Phys.* **2014**, *16*, 095001.
(255) Bryant, S. J.; Machta, B. B. Energy Dissipation Bounds in Autonomous Thermodynamic Systems. 2019, arXiv:1903.06780 [cond-mat.stat-mech]. arXiv.org e-Print archive. https://arxiv.org/abs/1903.06780.
(256) Erbas-Cakmak, S.; Leigh, D. A.; McTernan, C. T.; Nussbaumer, A. L. Artificial molecular machines. *Chem. Rev.* **2015**, *115*, 10081−10206.
(257) Wilson, M. R.; Sola, J.; Carlone, A.; Goldup, S. M.; Lebrasseur, N.; Leigh, D. A. An autonomous chemically fuelled small-molecule motor. *Nature* **2016**, *534*, 235−240.
(258) DelRosso, N. V.; Derr, N. D. Exploiting molecular motors as nanomachines: the mechanisms of de novo and re-engineered cytoskeletal motors. *Curr. Opin. Biotechnol.* **2017**, *46*, 20−26.
(259) Wang, Z.; Hou, R.; Loh, I. Y. Track-walking molecular motors: a new generation beyond bridge-burning designs. *Nanoscale* **2019**, *11*, 9240−9263.
(260) Hess, H. Engineering Applications of Biomolecular Motors. *Annu. Rev. Biomed. Eng.* **2011**, *13*, 429−450.
(261) McConnell, I.; Li, G.; Brudvig, G. W. Energy conversion in natural and artificial photosynthesis. *Chem. Biol.* **2010**, *17*, 434−447.
(262) Peng, H.; Li, X.-F.; Zhang, H.; Le, X. C. A microRNA-initiated DNAzyme motor operating in living cells. *Nat. Commun.* **2017**, *8*, 14378.
(263) Balzani, V.; Clemente-Leon, M.; Credi, A.; Ferrer, B.; Venturi, M.; Flood, A. H.; Stoddart, J. F. Autonomous artificial nanomotor powered by sunlight. *Proc. Natl. Acad. Sci. U. S. A.* **2006**, *103*, 1178−1183.
(264) Tierney, H. L.; Murphy, C. J.; Jewell, A. D.; Baber, A. E.; Iski, E. V.; Khodaverdian, H. Y.; McGuire, A. F.; Klebanov, N.; Sykes, E. C. H. Experimental demonstration of a single-molecule electric motor. *Nat. Nanotechnol.* **2011**, *6*, 625−629.
(265) Zuckermann, M. J.; Angstmann, C. N.; Schmitt, R.; Blab, G. A.; Bromley, E. H. C.; Forde, N. R.; Linke, H.; Curmi, P. M. G. Motor properties from persistence: a linear molecular walker lacking spatial and temporal asymmetry. *New J. Phys.* **2015**, *17*, 055017.
(266) Small, L. S. R.; Zuckermann, M. J.; Sessions, R. B.; Curmi, P. M. G.; Linke, H.; Forde, N. R.; Bromley, E. H. C. The bar-hinge motor: a synthetic protein design exploiting conformational switching to achieve directional motility. *New J. Phys.* **2019**, *21*, 013002.
(267) Kovacic, S.; Samii, L.; Curmi, P. M. G.; Linke, H.; Zuckermann, M. J.; Forde, N. R. Design and construction of the lawnmower, an artificial burnt-bridges motor. *IEEE Trans. Nanobioscience* **2015**, *14*, 305−312.
(268) Korosec, C. S.; Zuckermann, M. J.; Forde, N. R. Dimensionality-dependent crossover in motility of polyvalent burnt-bridges ratchets. *Phys. Rev. E: Stat. Phys., Plasmas, Fluids, Relat. Interdiscip. Top.* **2018**, *98*, 032114.
(269) Raz, O.; Subasi, Y.; Jarzynski, C. Mimicking nonequilibrium steady states with time-periodic driving. *Phys. Rev. X* **2016**, *6*, 021022.
(270) Astumian, R. D. Irrelevance of the power stroke for the directionality, stopping force, and optimal efficiency of chemically driven molecular machines. *Biophys. J.* **2015**, *108*, 291−303.

DOI: 10.1021/acs.chemrev.9b00254
Chem. Rev. 2020, 120, 434−459

(271) Maxwell, J. C. *Theory of Heat*; Appleton: London, 1871.
(272) Maruyama, K.; Nori, F.; Vedral, V. Colloquium: The physics of Maxwell's demon and information. *Rev. Mod. Phys.* **2009**, *81*, 1−23.
(273) Bennett, C. H. Notes on Landauer's principle, reversible computation and Maxwell's demon. 2002, arXiv:physics/0210005 [physics.class-ph]. arXiv.org e-Print archive. https://arxiv.org/abs/physics/0210005.
(274) Szilard, L. On the decrease of entropy in a thermodynamic system by the intervention of intelligent beings. *Eur. Phys. J. A* **1929**, *53*, 840−856.
(275) Parrondo, J. M. R.; Horowitz, J. M.; Sagawa, T. Thermodynamics of information. *Nat. Phys.* **2015**, *11*, 131−139.
(276) Landauer, R. Irreversibility and heat generation in the computing process. *IBM J. Res. Dev.* **1961**, *5*, 183−191.
(277) Bérut, A.; Arakelyan, A.; Petrosyan, A.; Ciliberto, S.; Dillenschneider, R.; Lutz, E. Experimental verification of Landauer's principle linking information and thermodynamics. *Nature* **2012**, *483*, 187−189.
(278) Jun, Y.; Gavrilov, M.; Bechhoefer, J. High-precision test of Landauer's principle in a feedback trap. *Phys. Rev. Lett.* **2014**, *113*, 190601.
(279) Bennett, C. H. The thermodynamics of computation — a review. *Int. J. Theor. Phys.* **1982**, *21*, 905−940.
(280) Horowitz, J. M.; Sagawa, T.; Parrondo, J. M. R. Imitating chemical motors with optimal information motors. *Phys. Rev. Lett.* **2013**, *111*, 010602.
(281) Toyabe, S.; Sagawa, T.; Ueda, M.; Muneyuki, E.; Sano, M. Experimental demonstration of information-to-energy conversion and validation of the generalized Jarzynski equality. *Nat. Phys.* **2010**, *6*, 988−992.
(282) Admon, T.; Rahav, S.; Roichman, Y. Experimental realization of an information machine with tunable temporal correlations. *Phys. Rev. Lett.* **2018**, *121*, 180601.
(283) Sagawa, T.; Ueda, M. Minimal energy cost for thermodynamic information processing: Measurement and information erasure. *Phys. Rev. Lett.* **2009**, *102*, 250602.
(284) Barato, A. C.; Seifert, U. Stochastic thermodynamics with information reservoirs. *Phys. Rev. E* **2014**, *90*, 042150.
(285) Hasegawa, H. H.; Ishikawa, J.; Takara, K.; Driebe, D. J. Generalization of the second law for a nonequilibrium initial state. *Phys. Lett. A* **2010**, *374*, 1001−1004.
(286) Sivak, D. A.; Crooks, G. E. Near-equilibrium measurements of nonequilibrium free energy. *Phys. Rev. Lett.* **2012**, *108*, 150601.
(287) Still, S.; Sivak, D. A.; Bell, A. J.; Crooks, G. E. Thermodynamics of prediction. *Phys. Rev. Lett.* **2012**, *109*, 120604.
(288) Quenneville, M.; Sivak, D. A. Energy dissipation and information flow in coupled Markovian systems. *Entropy* **2018**, *20*, 707−9.
(289) Hartich, D.; Barato, A. C.; Seifert, U. Stochastic thermodynamics of bipartite systems: transfer entropy inequalities and a Maxwell's demon interpretation. *J. Stat. Mech.: Theory Exp.* **2014**, *2014*, P02016.
(290) Barato, A. C.; Hartich, D.; Seifert, U. Efficiency of cellular information processing. *New J. Phys.* **2014**, *16*, 103024.
(291) Hartich, D.; Barato, A. C.; Seifert, U. Sensory capacity: An information theoretical measure of the performance of a sensor. *Phys. Rev. E: Stat. Phys., Plasmas, Fluids, Relat. Interdiscip. Top.* **2016**, *93*, 022116.
(292) Barato, A. C.; Hartich, D.; Seifert, U. Rate of mutual information between coarse-grained non-Markovian variables. *J. Stat. Phys.* **2013**, *153*, 460−478.
(293) Brittain, R. A.; Jones, N. S.; Ouldridge, T. E. What we learn from the learning rate. *J. Stat. Mech.: Theory Exp.* **2017**, *2017*, 063502.
(294) England, J. L. Statistical physics of self-replication. *J. Chem. Phys.* **2013**, *139*, 121923.
(295) England, J. L. Dissipative adaptation in driven self-assembly. *Nat. Nanotechnol.* **2015**, *10*, 919−923.
(296) Perunov, N.; Marsland, R. A.; England, J. L. Statistical physics of adaptation. *Phys. Rev. X* **2016**, *6*, 021036.
(297) Yu, H.; Jo, K.; Kounovsky, K. L.; de Pablo, J. J.; Schwartz, D. C. Molecular propulsion: Chemical sensing and chemotaxis of DNA driven by RNA polymerase. *J. Am. Chem. Soc.* **2009**, *131*, 5722−5723.
(298) Muddana, H. S.; Sengupta, S.; Mallouk, T. E.; Sen, A.; Butler, P. J. Substrate catalysis enhances single-enzyme diffusion. *J. Am. Chem. Soc.* **2010**, *132*, 2110−2111.
(299) Xu, M.; Valdez, L.; Sen, A.; Ross, J. L. Direct Single Molecule Imaging of Enhanced Enzyme Diffusion. 2018, arXiv:1811.08483 [q-bio.SC]. arXiv.org e-Print archive. https://arxiv.org/abs/1811.08483.
(300) Sengupta, S.; Dey, K. K.; Muddana, H. S.; Tabouillot, T.; Ibele, M. E.; Butler, P. J.; Sen, A. Enzyme molecules as nanomotors. *J. Am. Chem. Soc.* **2013**, *135*, 1406−1414.
(301) Illien, P.; Zhao, X.; Dey, K. K.; Butler, P. J.; Sen, A.; Golestanian, R. Exothermicity is not a necessary condition for enhanced diffusion of enzymes. *Nano Lett.* **2017**, *17*, 4415−4420.
(302) Riedel, C.; Gabizon, R.; Wilson, C. A. M.; Hamadani, K.; Tsekouras, K.; Marqusee, S.; Presse, S.; Bustamante, C. The heat released during catalytic turnover enhances the diffusion of an enzyme. *Nature* **2015**, *517*, 227−230.
(303) Gunther, J.-P.; Borsch, M.; Fischer, P. Diffusion measurements of swimming enzymes with fluorescence correlation spectroscopy. *Acc. Chem. Res.* **2018**, *51*, 1911−1920.
(304) Sengupta, S.; Spiering, M. M.; Dey, K. K.; Duan, W.; Patra, D.; Butler, P. J.; Astumian, R. D.; Benkovic, S. J.; Sen, A. DNA polymerase as a molecular motor and pump. *ACS Nano* **2014**, *8*, 2410−2418.
(305) Jee, A.-Y.; Dutta, S.; Cho, Y.-K.; Tlusty, T.; Granick, S. Enzyme leaps fuel antichemotaxis. *Proc. Natl. Acad. Sci. U. S. A.* **2018**, *115*, 14−18.
(306) Lynch, M. Evolution of the mutation rate. *Trends Genet.* **2010**, *26*, 345−352.

DOI: 10.1021/acs.chemrev.9b00254
Chem. Rev. 2020, 120, 434−459